Biomaterials 101 (2016) 321–340

Contents lists available at ScienceDirect

Biomaterials

journal homepage: www.elsevier.com/locate/biomaterials

Edible ginger-derived nanoparticles: A novel therapeutic approach for the prevention and treatment of inflammatory bowel disease and colitis-associated cancer

Mingzhen Zhang [a, b, *], Emilie Viennois [a, b], Meena Prasad [c, d], Yunchen Zhang [a, b], Lixin Wang [a, b, c], Zhan Zhang [a, b], Moon Kwon Han [a, b], Bo Xiao [a, b, e], Changlong Xu [a, b, f], Shanthi Srinivasan [c, d], Didier Merlin [a, b, c]

[a] Institute for Biomedical Sciences, Georgia State University, Atlanta, GA 30303, USA
[b] Center for Diagnostics and Therapeutics, Georgia State University, Atlanta, GA 30303, USA
[c] Veterans Affairs Medical Center, Decatur, GA, USA
[d] Emory University, Department of Medicine, USA
[e] Institute for Clean Energy and Advanced Materials, Faculty for Materials and Energy, Southwest University, Chongqing, 400715, PR China
[f] The 2nd Affiliated Hospital & Yuying Children's Hospital of Wenzhou Medical University, Wenzhou, 325027, PR China

ARTICLE INFO

Article history:
Received 28 March 2016
Received in revised form
2 June 2016
Accepted 7 June 2016
Available online 9 June 2016

Keywords:
Edible ginger derived nanoparticles
Inflammatory bowel disease
Colitis-associated cancer
Natural drug delivery system
Therapy

ABSTRACT

There is a clinical need for new, more effective treatments for chronic and debilitating inflammatory bowel disease (IBD), including Crohn's disease and ulcerative colitis. In this study, we characterized a specific population of nanoparticles derived from edible ginger (GDNPs 2) and demonstrated their efficient colon targeting following oral administration. GDNPs 2 had an average size of ~230 nm and exhibited a negative zeta potential. These nanoparticles contained high levels of lipids, a few proteins, ~125 microRNAs (miRNAs), and large amounts of ginger bioactive constituents (6-gingerol and 6-shogaol). We also demonstrated that GDNPs 2 were mainly taken up by intestinal epithelial cells (IECs) and macrophages, and were nontoxic. Using different mouse colitis models, we showed that GDNPs 2 reduced acute colitis, enhanced intestinal repair, and prevented chronic colitis and colitis-associated cancer (CAC). 2D-DIGE/MS analyses further identified molecular target candidates of GDNPs 2 involved in these mouse models. Oral administration of GDNPs 2 increased the survival and proliferation of IECs and reduced the pro-inflammatory cytokines (TNF-α, IL-6 and IL-1β), and increased the anti-inflammatory cytokines (IL-10 and IL-22) in colitis models, suggesting that GDNPs 2 has the potential to attenuate damaging factors while promoting the healing effect. In conclusion, GDNPs 2, nanoparticles derived from edible ginger, represent a novel, natural delivery mechanism for improving IBD prevention and treatment with an added benefit of overcoming limitations such as potential toxicity and limited production scale that are common with synthetic nanoparticles.

1. Introduction

Inflammatory bowel diseases (IBDs), which include ulcerative colitis and Crohn's disease, are chronic, debilitating inflammatory conditions for which existing treatments are largely limited by serious systemic side effects [1–3]. Over the last decade, the treatment options for IBD have been anti-inflammatory medications (5-amino salicylic acid, steroids) or immunosuppressants [4–6]. Despite the efficacy of these medications, further applications are limited by their non-specific actions on immune system that result in short- and long-term debilitating side effects, such as allergic reactions, nausea, elevated liver tests, pancreatitis, and other life-threatening side effects [7]. Furthermore, anti-inflammatory drugs that are locally active with minimal systemic absorption (5-aminosalicylates) require frequent high-dose administration to exert measurable clinical efficacy. Moreover, while sustained drug-release devices, such as pellets, capsules or tablets, designed to deliver drugs specifically to the colon for longer

* Corresponding author. Center for Diagnostics and Therapeutics, Institute for Biomedical Science, Georgia State University, Atlanta, 30303, USA.
E-mail address: mzhang21@gsu.edu (M. Zhang).

http://dx.doi.org/10.1016/j.biomaterials.2016.06.018
0142-9612/

periods of time have been developed, these drugs have limited therapeutic efficacy and are effective in only a subset of IBD patients [8–13].

More recently, targeted therapeutic approaches, based on the pathophysiology of inflammatory responses in IBD, have been developed. These therapeutic strategies can be divided into three categories: development of inhibitors of inflammatory cytokines, such as tumor necrosis factor (TNF)-α, that induce T-lymphocyte apoptosis; identification of anti-inflammatory cytokines that down-regulate T-lymphocyte proliferation; and synthesis of selective adhesion molecule inhibitors that suppress T-lymphocyte trafficking into the gut epithelium. Anti-TNF-α agents are among the most potent drugs in the treatment of IBD. However, they must be administered systemically and their use is limited by serious side effects [14]. Thus, there is an unmet need for a carrier system capable of delivering drugs specifically and exclusively to the inflamed regions for a prolonged period of time. Such a system could significantly reduce the side effects of existing, otherwise effective, treatments.

To address this formidable challenge, targeting drug carriers based on nanoparticles have been designed and have shown great promises for improving IBD treatment. Various carriers have been designed to release the drug at a specific pH value, to be resistant to digestive enzymes, and/or require bacterial cleavage for activation, in which several of these carriers are currently being investigated. Our laboratory and others have recently demonstrated that artificially synthesized nanoparticles can be used to deliver low doses of drugs to specific cell types and tissues, and decrease the systemic side effects of medications [15–26]. However, the nanoparticles synthesized to date have two major limitations: i) each constituent of the synthesized nanoparticles must be examined for potential *in vivo* toxicity before clinical application; and ii) the production scale is limited. In contrast, nanoparticles derived from natural sources are considered to be safe and cost effective that may overcome aforementioned limitations of synthetic nanoparticles [27]. Recently, exosome-like nanoparticles isolated from edible plants using an eco-friendly protocol have been characterized [28]. These nature-derived nanoparticles could serve interspecies communication roles and exert anti-inflammatory properties in IBD treatment [29–31]. These observations suggest that the application of plants as “nanofactories” for the fabrication of medical nanoparticles could represent a new approach for IBD treatment.

Ginger, the rhizome of *Zingiber officinale*, is one of the most widely used natural products. It is consumed as a spice and used as a medicine for the treatment of nausea, as well as other digestive tract problems like colic, flatulence, diarrhea and dyspepsia [32–35]. Studies have also shown that ginger and its active components, including 6-gingerol and 6-shogaol, exert anti-oxidative, anti-inflammatory, and anti-cancer activities [36–38]. In the present study, we assessed the feasibility of isolating ginger-derived nanoparticles, characterized their properties, and examined their potential use as a new treatment for IBD and CAC.

2. Materials and methods

2.1. Chemicals

The fluorescent lipophilic dyes, 1,1′-dioctadecyl-3,3,3′,3′-tetramethylindocarbocyanine perchlorate (DiL), 3,3′-dioctadecyloxacarbocyanine perchlorate (DiO) and 1,1′-dioctadecyl-3,3′,3′-tetramethylindotricarbocyanine iodide (DiR), were purchased from Promokine (Heidelberg, Germany); DC-Chol/DOPE Blend was from Avanti Polar Lipids (Alabaster, AL, USA); phalloidin-FITC, O-dianisidine dihydrochloride, myeloperoxidase from human leukocytes, type VIII collagenase, DNase I, (6)-gingerol and (6)-shogaol standards were purchased from Sigma (St. Louis, MO, USA). Rabbit anti-mouse E-cadherin antibody was from Santa Cruz Biotechnology (Santa Cruz, CA, USA). Anti-mouse CD326 (EpCAM) PE-Cy7, anti-mouse CD11b eFluo 450; anti-mouse CD11c APC, and anti-mouse F4/80 antigen PE-Cy7 were purchased from eBioscience (San Diego, CA, USA). Duoset enzyme-linked immunosorbent assay (ELISA) kits were purchased from R&D Systems (Minneapolis, MN, USA).

2.2. Isolation, purification, and characterization of ginger-derived nanoparticles (GDNPs)

For isolation of GDNPs, ginger or Zingiber officinale (Family, Zingiberaceae; Order, Zingiberales; Superorder, Lilianae; Subclass, magnoliidae; Class, Equisetopsida) was purchased from a local farmers' market. The utilized ginger was purchased from three different farmers' markets in Atlanta, Georgia; More than 20 batches were purchased over the past 12 months. Results similar to those reported in the manuscript were obtained using these different ginger batches from different sources. Ginger was washed thoroughly with tap water at room temperature (22 °C). After the final washing, the ginger was ground in a blender to obtain juice, then the juice was centrifuged first at 3000*g* for 20 min and then at 10,000*g* for 40 min to remove large ginger fibers. The supernatant was ultracentrifuged at 150,000*g* for 2 h, and the pellet was suspended in phosphate-buffered saline (PBS) through ultrasonic dispersion.

For purification of GDNPs, the suspension was transferred to a discontinuous sucrose gradient (8%, 30%, 45% and 60% [g/v]) and ultracentrifuged at 150,000*g* for an additional 2 h. The bands between 8/30%, 30/45%, and 45/60% layers, which corresponds to GDNPs 1, GDNPs 2 and GDNPs 3, respectively, were harvested. The concentrations of the GDNPs obtained were quantified based on protein concentration using a Bio-Rad protein quantification assay kit. The quantified GDNPs were stored at −80 °C until use.

GDNPs were characterized with respect to size and zeta potential by dynamic light scattering using 90 Plus/BI-MAS (multi-angle particle sizing) or dynamic light scattering after applying an electric field using a ZetaPlus instrument (Brookhaven Instruments Corp, Holtsville, NY, USA). Atomic force microscopy (AFM) images were acquired using an SPA 400 AFM instrument (Seiko Instruments Inc., Chiba, Japan). For transmission electron microscopy (TEM) imaging, a drop of sample was deposited onto the surface of a formvar-coated copper grid, after which 1% uranyl acetate was added for 15 s and the sample was allowed to dry at room temperature for subsequent imaging.

For *in vitro* stability tests, 1.34 μl of 18.5% (w/v) HCl (pH 2.0) and 24 μl of pepsin solution (80 mg/ml in 0.1 N HCl, pH 2.0) were added to 1 ml (1 mg/ml) of GDNPs in PBS, and the mixture was incubated at 37 °C for 0.5 h (stomach-like conditions). Then, 80 μl of a mixture containing 24 mg/ml of bile extract and 4 mg/ml of pancreatin in 0.1 N $NaHCO_3$ was added. The pH was adjusted to 6.5 with 1 N $NaHCO_3$ and incubated for an additional 0.5 h under the same conditions (intestine-like). The stability of GDNPs was evaluated by measuring particle size and zeta potential using the method described above.

2.3. Lipids, proteomics, and microRNA sequencing discovery of GDNPs

For lipidomic analyses, lipid samples extracted from band 1, 2 and 3 were submitted to the Lipidomics Research Center, Kansas State University (Manhattan, KS, USA) for analysis. Briefly, the lipid composition of GDNPs was determined using a triple quadrupole

mass spectrometer (Applied Biosystems Q-TRAP; Applied Biosystems, Foster City, CA, USA), as described in an online protocol (http://www.k-state.edu/lipid/lipidomics/profiling.htm). Data for each lipid molecular species were presented as mol % of the total lipids analyzed.

For proteomics analysis of GDNPs 2, samples on dry ice were shipped to Bioproximity (Chantilly, VA, USA). GDNPs proteins were identified and quantified by UPLC-MS/MS (ultra-performance liquid chromatography tandem mass-spectrometry) using Orbitrap mass spectrometry.

For sequencing discovery of GDNPs, total RNA for GDNPs 2 was isolated in duplicates using a Urine Exosome RNA Isolation kit (Cat# 47200; Norgen Biotek, Thorold, ON, Canada) according to the manufacturer's instructions. The purified RNA sample was processed to generate a cDNA library that was then used for deep sequencing.

2.4. Cell culture

RAW 264.7 cells, Caco-2BBE, and Colon-26 cells were cultured to confluency in 75-cm^2 flasks at 37 °C in a humidified atmosphere containing 5% CO_2. RAW 264.7 and Caco-2BBE cells were cultured in Dulbecco's Modified Eagle Medium (DMEM), and Colon-26 cells were cultured in RPMI 1640 medium (Life Technologies, Grand Island, NY, USA), in which both cases were supplemented with penicillin (100 U/ml), streptomycin (100 U/ml), and heat-inactivated fetal bovine serum (10%) (Atlanta Biological, Lawrenceville, GA, USA).

2.5. GDNPs labeling

GDNPs were labeled with the fluorescent lipophilic dyes, DiL, DIO or DiR, depending on the experiment. Generally, 10 μM dye solution was added to 1 mg GDNPs (1 ml in PBS), and the mixture was incubated for 30 min at room temperature. The labeled GDNPs were then passed through a 100-kDa ultracentrifuge filter to remove the free dye.

2.6. In vitro internalization of GDNPs

RAW 264.7 microphage and Colon-26 cells were seeded in 8-chamber glass tissue culture slides (BD Falcon, Bedford, MA, USA) at a density of 1×10^5 cells/well and incubated overnight in growth medium. GDNPs 2 were labeled with DiL (Ex: 549 nm; Em: 565 nm) at a concentration of 10 μM. Subsequently, labeled GDNPs 2 (50 μg/ml) were incubated with cells for 4 h. After incubation, cells were fixed with 4% paraformaldehyde (PFA) for 10 min, and then dehydrated with acetone at −20 °C for 5 min. After blocking with 1% bovine serum albumen (BSA) in PBS for 30 min, 100 μl of phalloidin-FITC (1:40 dilution) was added and the mixture was incubated for an additional 30 min. Finally, cells were coverslip-mounted with mounting medium containing 4-,6-diamidino-2-phenylindole (DAPI, H-1500; Vector Laboratories, Burlingame, CA, USA). Cells were observed and imaged using a Zeiss LSM 700 confocal microscope with Zen 2014 software version 9.1.

2.7. Cytotoxicity assay

For MTT [3-(4,5-dimethythiazol-2-yl)-2,5-diphenyl tetrazolium bromide] cell proliferation assay, RAW 264.7 microphages and Colon-26 cells were seeded in 96-well plates at a density of 1×10^4 cells/well and incubated overnight. Cells were then incubated with different amounts of GDNPs 2 (1, 10, 20, 50, 100 μg) in PBS for 24 h, after which the GDNPs 2-containing medium was removed and cells were thoroughly rinsed once with PBS. Cells were then incubated with 20 μl of MTT (5 mg/ml) containing phenol red free medium at 37 °C for 4 h until a purple precipitate was visible. Thereafter, the media were discarded and 50 μl dimethyl sulfoxide (DMSO) was added to each well prior to spectrophotometric measurements at 570 nm. Untreated cells were used as a negative control.

Barrier function assays were performed using ECIS (electric cell-substrate impedance-sensing) technology (Applied Biophysics, Troy, NY, USA). Before starting, the Trans-Filter Array system was sterilized with 75% ethanol under a cell culture hood for 30 min, after which 1 ml medium was added to each array well. The insert, seeded with 2×10^5 Caco-2BBE cells in 500 μl medium, was then transferred into the array plate with sterilized forceps. After a monolayer of cells had formed, PBS or GDNPs 2 (0.1 mg/ml) was added to the well. Cell resistance was continuously measured for 120 h.

The annexin V-FITC/propidium iodide apoptosis assay was used to quantify cell apoptosis and death *in vitro*. Colon-26 and RAW 264.7 macrophage cells were plated in 12-well culture plates and cultured in the presence of different concentrations of GDNPs 2 (1, 10, 20, 50 and 100 μg) for 24 h. At the end of culture period, cells were washed twice with cold PBS and then suspended in annexin V binding buffer at a cell concentration of 1×10^6 cells/mL. Subsequently, 100 μl of cells suspension were transferred to a 5 ml culture tube in which 5 μl annexin V-FITC and 5 μl PI were added and incubated at RT for 15 min in the dark. Finally, 400 μl of annexin V binding buffer were added to the tube for the analysis. Unstained cells and cells stained with FITC or PI were also prepared in parallel.

2.8. Wound-healing assay

Healing of wounded intestinal epithelial monolayers by GDNPs 2 (0.1 mg/ml) was performed using ECIS technology (ECIS model 1600R; Applied BioPhysics). The ECIS device is based on AC impedance measurements using weak and noninvasive AC signals, as previously described. The attachment and spread of cells on the electrode surface change the impedance in such a way that morphological information about attached cells can be inferred. The measurement system consists of an 8-well culture dish (ECIS 8W1E plate) with the surface treated for cell culture. The bottom of each well contains a small, active electrode and a large counter electrode. A lock-in amplifier with an internal oscillator is used to switch among the different wells, and a personal computer controls the measurement and stores the data. Once cells reached confluency, PBS, GDNPs 2, or DC-Chol/DOPE liposome (with the same lipid concentration as GDNPs 2) was added. For wounding, monolayers grown on ECIS 8W1E plates were subjected to a 30 s pulse with a frequency of 40 kHz and amplitude of 4.5 V. Basal resistance was measured at a frequency of 500 Hz and a voltage of 1 V.

2.9. Mice

Female C57BL/6 or FVB/NJ mice (6–8 wk old) were purchased from Jackson Laboratories (Bar Harbor, ME, USA). Mice were housed under specific pathogen-free conditions. All the experiments involving mice were approved by the institutional animal care and use committee (IACUC) of Georgia State University (Atlanta, GA, USA).

2.10. DSS-induced colitis mouse model

Colitis was induced in FVB/NJ mice by adding 1.5% (w/v) dextran sodium sulfate (DSS; 36–50 kDa; MP Biomedicals (Santa Ana, CA, USA) in drinking water for 7 d. Mice in the GDNPs treatment group were also orally administered GDNPs (0.3 mg/mouse) every day for

the duration of the study, whereas untreated animals served as controls. The DSS solution was freshly prepared every other day. Body weight, feces, and physical activity were monitored daily. After 7 d, mice were euthanized with CO_2, in which spleen and colon were harvested for measurements.

2.11. DSS-induced colitis wound healing

In this model, mice in both DSS and GDNPs 2 treatment groups were first subjected to 7 d of 1.5% DSS water. Then, both groups were changed to regular water for an additional 7-d wound-healing period; mice in the GDNPs 2 treatment group were orally administered GDNPs 2 (0.3 mg/mouse) every day at the same time. Body weight, feces, and physical activity were monitored daily.

2.12. $IL10^{-/-}$ spontaneous colitis model

Female C57BL/6 and $IL10^{-/-}$ mice (3 wk old) were obtained from Jackson Laboratories. Untreated $IL10^{-/-}$ mice (control group) spontaneously develop colitis. For the GDNPs 2 treatment group, $IL10^{-/-}$ mice were orally administered GDNPs 2 (0.3 mg/mouse) every day from 4 wk of age to the end of the experiment. Mice were monitored for 19 weeks for the development of colitis.

2.13. Colitis-associated cancer model

Colitis-associated cancer (CAC) was induced as previously described, with some modifications. Briefly, mice were intraperitoneally injected with Azoxymethane (AOM) (10 mg/kg body weight) and maintained with regular water and diet for 7 d. Mice were then subjected to two cycles of DSS treatment, each consisting of 2% DSS for 7 d followed by a 14-d recovery period with regular water. In the GDNPs 2 treatment group, mice were orally administered GDNPs (0.3 mg/mouse) every day throughout the experiment. At the end of the experiment, colonic tumors were counted and measured using a dissecting microscope.

2.14. Biodistribution and cellular targeting of oral administrated GDNPs 2

To investigate the *in vivo* biodistribution of GDNPs 2, fasted and unfasted mice were given a single oral dose of DiR-labeled GDNPs 2 (0.3 mg/ml). At different time points after gavage (2, 4, 6, 12, and 24 h), mice were killed and colon tissues were harvested for fluorescence imaging using an IVIS Spectrum Series *in vivo* imaging system.

2.15. Isolation of intestinal epithelial cells, dendritic cells, and microphages from colons and analysis by flow cytometry

Intestinal epithelial cells ($EpCAM^+$ cells), dendritic cells ($Cd11c^+$ cells), and microphages ($Cd11b^+F4/80^+$ cells) were isolated as described previously. Six hours after oral administration of DiO-labeled GDNPs 2, colons from mice with or without DSS treatment were removed, carefully cleaned of their mesentery, opened longitudinally, and washed of feces. Colons were then cut into pieces 0.5 cm in length, which were transferred into 50-ml tubes and shaken at 250 rpm for 20 min at 37 °C in Hanks balanced salt solution (HBSS) supplemented with 5% FBS and 2 mM EDTA. This process was repeated once, and then cell suspensions were passed through 100-μm and 40-μm strainers. Finally, the epithelial cells ($EpCAM^+$ cells) were collected by centrifugation at 1500 rpm for 5 min at 4 °C.

For isolation of dendritic cells ($Cd11c^+$ cells) and microphages ($Cd11b^+F4/80^+$ cells), the remaining tissue was washed, minced, transferred to a 50-ml conical tube, and shaken for 15 min at 37 °C in HBSS containing 5% FBS, type VIII collagenase (1.5 mg/ml; Sigma), and DNase I (40 μg/ml; Sigma). Cell suspensions were collected and passed through 100-μm and 40-μm strainers, and pelleted by centrifugation at 1500 rpm for 5 min at 4 °C.

For flow cytometry, 1×10^6 cells in fluorescence-activated cell sorting (FACS) buffer (Santa Cruz Biotechnology, Inc., Dallas, USA) were transferred into a 96-well plate (Fisher 12,565,503). After blocking cells with FcrRIIbCD16-2 antibody for 10 min at 4 °C, the cells were stained with labeled antibodies at 4 °C for 30 min. Cells were then washed twice with FACS buffer for immediate analysis or were fixed with 2% PFA and stored at 4 °C. The following antibodies used for analysis were purchased from eBioscience (San Diego, CA, USA): anti-mouse CD326 PE-Cy7 (EpCAM), anti-mouse CD11b eFluo 450, anti-mouse CD11c APC, and anti-mouse F4/80 antigen PE-Cy7. Flow cytometry analyses were performed on a BD LSRFortessa flow cytometer (BD Biosciences) and data were analyzed using FlowJo software.

2.16. Histological analyses of tissue sections by hematoxylin and eosin staining

Mice colons and different organs were fixed in 10% formalin for 24 h or longer at room temperature, then embedded in paraffin. Tissues were sectioned at 6 μm thickness and stained with hematoxylin and eosin (H&E) using standard protocols established in our own lab. Images were acquired using an Olympus microscope equipped with a DP-26 digital camera.

2.17. Immunofluorescence

Paraffin-embedded tissues (6 μm thick) were deparaffinized, epitope retrieved, and blocked by incubating with goat serum for 45 min at room temperature. The sections were covered with rabbit anti-mouse E-cadherin antibody (Santa Cruz Biotechnology; sc-7870), diluted 1:50 in PBS, and incubated for 1 h at room temperature. Sections were washed with PBS, and incubated with Alexa Fluor 488-conjugated anti-rabbit secondary antibody (1:200 dilution; Life Technologies) for 1 h at room temperature, and coverslip-mounted with mounting medium containing DAPI (Vector Laboratories; H-1500). Sections were viewed under an Olympus fluorescence microscope, and images were acquired with a Hamamatsu digital camera (Orca-03G).

2.18. Immunohistochemistry

For staining with the proliferation marker Ki67, 6-μm-thick paraffin-embedded tissue sections were deparaffinized in xylene, incubated in 3% hydrogen peroxide in PBS for 30 min, then treated with 10 mM sodium citrate buffer (pH 6.0) containing 0.05% Tween 20 and heated in a pressure cooker for 10 min (antigen retrieval). Sections were blocked with goat serum for 45 min at 37 °C, followed by incubation with anti-Ki67 antibody (1:50; Vector Laboratories) for 1 h at 37 °C. After washing with PBS containing 0.01% Tween 20, sections were incubated first with the appropriate biotinylated secondary antibody for 30 min at 37 °C, and then with reagents from the Vectastain ABC kit (Vector Laboratories) to allow color development. Sections were counterstained with hematoxylin, dehydrated, and coverslip-mounted. Images were acquired using an Olympus microscope equipped with a DP-26 digital camera.

2.19. TUNEL assay

Colon sections were deparaffinized, and apoptotic cells were

detected by immunofluorescence TUNEL (terminal deoxynucleotidyl transferase-mediated deoxyuridine triphosphate nick-end labeling) assay using the In Situ Cell Death Detection Kit (Roche Diagnostics, Indianapolis, IN, USA). Detailed protocol is provided in Methods and Materials in Supporting Information. Images were acquired using an Olympus microscope equipped with a Hamamatsu ORCA03G digital camera.

2.20. Myeloperoxidase assay

Colon tissues were homogenized in pre-chilled potassium phosphate buffer (50 mM K_2HPO_4 and 50 mM KH_2PO_4, pH 6.0) containing 0.5% hexadecyltrimethylammonium bromide (HTAB; Sigma). The homogenates were then sonicated, subjected to three freeze-thaw cycles (10 min/10 min), and centrifuged at 14,000 rpm for 15 min. The clarified supernatants were collected. O-Dianisidine dihydrochloride (1 mg/ml) and 0.0005% H_2O_2 were added to supernatants (50 μl) or myeloperoxidase (MPO) standards, and the change in absorbance at 460 nm was measured before saturation. One unit of MPO activity was defined as the amount that degraded 1 μmol of peroxidase per minute.

2.21. Quantification of fecal Lcn-2

Freshly collected or frozen fecal samples which were dried in an oven at 37 °C in advance were reconstituted in PBS containing 0.1% Tween 20 (100 mg/ml) and vortexed for 20 min to yield a homogeneous fecal suspension. Samples were then microcentrifuged for 10 min at 4 °C at full speed, and supernatants were collected for analysis. Levels of Lcn-2 were estimated using a Duoset mouse Lcn-2 ELISA kit (R&D Systems).

2.22. RNA extraction and real-time reverse transcription-polymerase chain reaction

Total RNA was extracted from colon tissues using an RNeasy mini Kit (Qiagen, Valencia, CA, USA) according to the manufacturer's instructions. Yield and quality of extracted RNA were verified with a Synergy 2 plate reader (BioTek, Winooski, VT, USA). cDNA was generated from the total RNA isolated above using a Maxima First-Strand cDNA Synthesis kit (Thermo Scientific, Lafayette, CO, USA). Expression of target mRNAs was quantified by real-time reverse transcription-polymerase chain reaction (qRT-PCR) using Maxima SYBR green/ROX (6-carboxyl-X-rhodamine) qPCR Master Mix (Thermo Scientific) and the following primer pairs: IL-10, 5′-GGT TGC CAA GCC TTA TCG GA-3′ (forward) and 5′-CTT CTC ACC CAG GGA ATT CA-3′ (reverse); IL-6, 5′-ACA AGT CGG AGG CTT AAT TAC ACA T-3′ (forward) and 5′-TTG CCA TCC GCA CAA CTC TTT TC-3′ (reverse); IL-1β, 5′-TCG CTCA GGG TCA CAA GAA A-3′ (forward) and 5′-CAT CAG AGG CAA GGA GGA AAA C-3′ (reverse); TNF-α, 5′-AGG CTG CCC CGA CTA CGT-3′ (forward) and 5′-GAC TTT CTC CTG GTA TGA GAT AGC AAA-3′ (reverse); cyclin D, 5′-CAG ACG TTC AGA ACC AGA TTC-3′ (forward) and 5′-CCC TCC AAT AGC AGC GAA AAC-3′ (reverse); and 36B4, 5′-TCC AGG CTT TGG GCA TCA-3′ (forward) and 5′-CTT TAT CAG CTG CAC ATC ACT CAG A-3′ (reverse).

2.23. Colon organ culture and cytokine analysis

Local levels of IL-10, IL-22, IL-6, IL-1β and TNF-α were assessed by first washing colon tissues from different treatment groups with PBS containing penicillin/streptomycin and then cutting them into 1-cm-long sections. Colon sections were cultured in serum-free RPMI 1640 medium supplemented with penicillin/streptomycin for 24 h, after which cell-free supernatants were harvested and assayed for cytokine secretion using Duoset cytokine ELISA kits (R&D Systems).

2.24. 2D-DIGE gel

Colon tissues from different mouse models (DSS with/without GDNPs 2 treatment; DSS wound healing with/without GDNPs 2 treatment; AOM/DSS with/without GDNPs 2 treatment [tumor tissue and normal tissue]) were analyzed by comparative proteomics using 2D-DIGE (two dimensional-differences in gel electrophoresis). Colon tissue samples were homogenized in ToPI-DIGE buffer, and the lysate was transferred to a new tube after centrifugation. Protein concentration was determined using the ToPA Bradford Protein Assay. Thereafter, 50 μg of each sample was labeled with 200 pmole Cy3 or Cy5 dye. A pooled sample containing 25 μg of each sample was labeled with Cy2 and used as a pooled standard (PS) to enable comparisons of samples on different gels. The samples were loaded onto 24-cm isoelectric focusing (IEF) strips (pH 3–10, non-linear). The strips were rehydrated in sample-containing solutions for 12 h at 30 V. The rehydrated IEF strips were focused for a total of 65,000 V-hours, and then were loaded onto a 24 cm × 20 cm, 12.5% SDS-PAGE gel, and ran for 4 h. Thereafter, the gel was scanned using a Typhoon Digital Imager at three different wavelengths. The images were analyzed using DeCyder Difference In-Gel Analysis (DIA) and Biological Variation Analysis (BVA) software (GE Healthcare, Atlanta, GA, USA), and candidate spots corresponding to differentially expressed proteins were identified and selected based on a volume ratio threshold of 2.0 or greater.

For spot identification, 2D-DIGE gels were stained with Lava Purple Gel stain in order to obtain a more accurate spot map for picking the gel spots of interest. Then the spots were de-stained and digested overnight with trypsin. The digest was then extracted from the gel plugs and dried down. Subsequently, the digests were re-suspended and desalted with a Ziptip and then dried again. Finally, the dried samples were re-suspended in 2% acentonitrile/0.1% formic acid and injected into a picofrit C18 nanospray column for mass spec analysis.

2.25. High-performance liquid chromatography with mass-spectrometric detection

All samples were analyzed using an HPLC-MS method (Agilent 6410 series) employing a positive ionization mode with multiple reaction monitoring (MRM) of 6-gingerol and 6-shogaol. The ion spray voltage was set at 3000 V, ionization temperature was set at 200 °C, and drying gas flow rate was 10 μl/min. Data acquisition and quantification were performed using Mass Hunter software (Agilent Technologies, Wilmington, DE, USA). Separation was achieved using an HP1100 series LC system (Agilent Technologies) equipped with a photodiode array detector using an Agilent Zorbax reversed-phase column (SB-C18, 3.0 × 250 mm, 5.0 μm). A gradient method was employed to separate the individual ginger components using mobile phase A (0.1% formic acid in water) and mobile phase B (acetonitrile). The gradient elution process was set to 60% B at 0 min, 90% B at 20 min, hold for 10 min and return to 60% B at 40 min, with a flow rate of 0.4 ml/min. An injection volume of 10 μl was used for analyses.

2.26. Statistical analyses

One-way and two-way analyses of variance (ANOVA) and *t*-tests were used to determine statistical significance ($^{*}p < 0.05$, $^{**}p < 0.01$, $^{***}p < 0.0001$).

3. Results

3.1. Characterization of GDNPs

GDNPs were isolated from ginger juice and purified using a

sucrose gradient ultracentrifugation method [28]. As shown in Fig. 1A, GDNPs mainly accumulated at the 8/30% (band 1) and 30/45% (band 2) interfaces of the sucrose gradient; a faint band was also detected at the 45/60% interface (band 3). The size distributions and zeta potentials of GDNPs were determined using photon correlation spectroscopy (PCS) employing Brookhaven equipment (Supplementary Fig. 1). The average size was about 292.5 nm for nanoparticles found in band 1, 231.6 nm for those from band 2, and 219.6 nm for those from band 3. A zeta potential value of approximately −12 mV at pH 6 (the pH of the duodenum-jejunum) was obtained for GDNPs from bands 1 (GDNPs 1) and 2 (GDNPs 2). In contrast, a zeta potential close to zero (about −2.1 mV) was obtained for band 3 nanoparticles (GDNPs 3). We also found that GDNPs 1 and GDNPs 2 (but not GDNPs 3) could tolerate freeze/thaw cycles and were very stable at room temperature (up to 7 days). Based on this finding, GDNPs 3 were excluded from subsequent analyses because of their lower yield and instability. We also used transmission electron microscopy (TEM) and atomic force microscopy (AFM) to characterize GDNPs 1 (Fig. 1B, C) and GDNPs 2 (Fig. 1D, E). These TEM and AFM data confirmed that the integrity and size of GDNPs were consistent with those measured using the PCS technique. Importantly, from a starting material of 1000 g ginger, we obtained ~50 mg of GDNPs from bands 1, 2 and 3. A consistent yield was observed across different ginger batches, and it represented a high-level of GDNPs production compared to the synthesis of nanoparticles. We thus successfully isolated and characterized two stable populations of nanoscale GDNPs.

3.2. Biochemical characterization of GDNPs

The total lipid composition of the GDNPs from these three bands showed slight differences (Supplementary Fig. 2 and Supplementary Table 1), but a composition analysis revealed mainly phosphatidic acid (~25–40% of total lipids), digalactosyldiacylglycerol (~25–40% of total lipids) and monogalactosyldiacylglycerol (~20–30% of total lipids). We also examined the protein composition of GDNPs 1, GDNPs 2, and GDNPs 3 using proteomic profiling assays, in which ultra-high-pressure liquid chromatography (HPLC) was coupled to high-resolution, high-mass accuracy quadrupole-orbitrap mass spectrometry (MS; Thermo Scientific Q-Exactive). We found that GDNPs had a low protein content, which tended to be predominantly cytosolic, such as actin and proteolysis enzymes, with a few membrane proteins, such as membrane channel/transporters (*e.g.*, aquaporin and chloride channels) (Supplementary Table 2**)**. To assess the presence or absence of microRNAs (miRNAs) in GDNPs, we extracted total RNA and generated cDNA libraries. Deep sequencing revealed that there were 125 different miRNAs in GDNPs 2, each containing between 15 and 27 nucleotides (Supplementary Table 3**)**. Targetscan (www.targetscan.org), which is an online software provided by the Whitehead Institute for prediction of microRNA targets, showed that 124 of these miRNAs could potentially target and regulate the expression of human genes by binding to their 3'-untranslated regions (3'-UTRs). Taken together, these findings demonstrate that our preparations isolated from ginger are exosome-like nanoparticles.

Ginger was chosen in this study because of its active constituents, including 6-gingerol and 6-shogaol, which have multiple molecular targets, including inflammatory mediators [36–38]. Using HPLC/MS we found that GDNPs 2 contain higher concentrations of the ginger active constituents, 6-gingerol (5.68 μg/mg) and 6-shogaol (2.95 μg/mg) compared with GDNPs 1 (0.56 and 0.22 μg/mg 6-gingerol and 6-shogaol, respectively) (Fig. 2). This latter observation demonstrates that GDNPs 1 and GDNPs 2 may have their own specific biochemical characteristics.

3.3. GDNPs are stable in stomach- and intestine-like solutions

Next, we determined whether these GDNPs are stable in stomach- and intestine-like solutions. We first mimicked *in vivo*

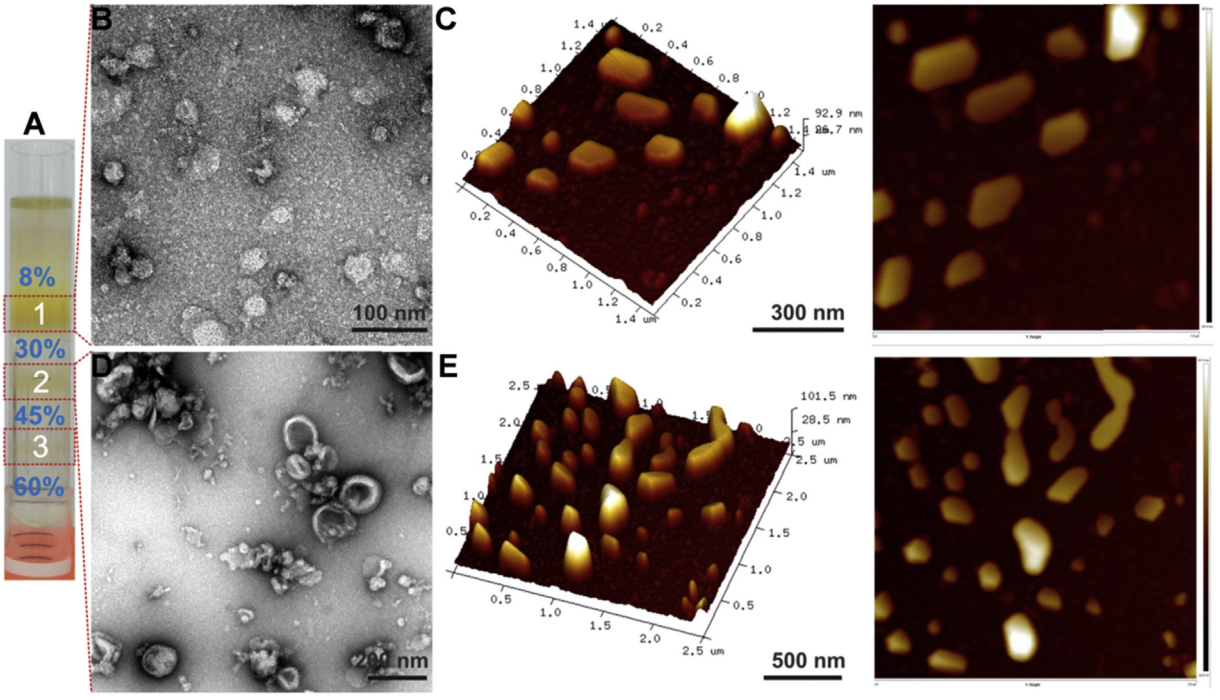

Fig. 1. Characterization of GDNPs. (A) Three bands formed after sucrose gradient ultracentrifugation. Band 1 from the 8/30% interface (GDNPs 1) was visualized by TEM (B) and AFM (C). Band 2 from the 30/45% interface (GDNPs 2) was visualized by TEM (D) and AFM (E).

conditions by suspending GDNPs 2 in phosphate-buffered saline (PBS) or a stomach- or intestine-like solution, and then analyzed changes in their size and zeta potential (Supplementary Fig. 3). The results showed that the size of GDNPs 2 was reduced slightly in both stomach- and intestine-like solutions compared with that in PBS. Zeta potential changed according to the pH value: in a near-neutral pH solution (PBS) and intestine-like solution, the surface of GDNPs 2 was negatively charged (−14.2 mV and −7.3 mV respectively), whereas in an acid environment (stomach-like solution), GDNPs 2 were weakly positively charged (0.26 mV). We also obtained similar results for GDNPs 1 (data not shown). Together, these data indicate that GDNPs are highly stable in both stomach-like and intestine-like solutions, and changes in their zeta potential coincide with the natural properties of GDNPs.

3.4. Oral administration of colon-targeting GDNPs

Oral administration of GDNPs has several advantages (such as convenience with no need for sterilization) over other therapeutic routes. Our primary goal was to deliver GDNPs to the colon, the site of intestinal inflammation in ulcerative colitis. Accordingly, mice were fed normally or starved for 12 h (Supplementary Fig. 4), and then orally administered DiR dye-labeled GDNPs 2. At 12 h post-treatment, the stomach, small intestine and colon were imaged. Control non-starved mice were orally administered PBS. In non-starved mice, images showed low-intensity GDNPs 2 signals in the stomach and small intestine, indicating low levels of localization in these tissues, but exhibited high-intensity signals in the colon. In starved mice, by contrast, retention of GDNPs 2 in the stomach and small intestine was more prominent, whereas colonic retention was less pronounced. Similar results were obtained in mice gavaged with GDNPs 1. Overall, these results indicate that retention of orally administered GDNPs in the colon is higher in non-starved mice than in starved mice. This preferential colon targeting is important for the potential use of GDNPs in IBD treatment.

3.5. Oral administration of GDNPs 2 reduces the susceptibility of mice to DSS-induced colitis

To assess the anti-inflammatory actions of GDNPs in the colon, we investigated the effects of GDNPs 1 and GDNPs 2 in the mouse model of dextran sulfate sodium (DSS)-induced acute colitis with ulceration, a well-established mice model for the study of human ulcerative colitis [39]. To this end, mice in GDNPs treatment groups were provided only DSS water (1.5% w/v) for 7 days and were simultaneously orally administered 0.3 mg GDNPs 1 or GDNPs 2 daily for the entire treatment period; mice provided plain water or DSS water (1.5% w/v) without GDNPs treatment served as controls. To assess the progression of intestinal inflammation in different treatment groups (water only, DSS only, DSS + GDNPs 1 and DSS + GDNPs 2), we measured the levels of lipocalin-2 (Lcn-2), a widely accepted biomarker for intestinal inflammation [55], in samples obtained daily during the treatment using ELISAs. As shown in Fig. 3A, basal Lcn-2 levels in the different treatment groups were similarly low on Day 1; however, Lcn-2 levels dramatically increased from Day 3 to Day 7 (with similar kinetics) in mice treated with DSS and DSS + GDNPs 1. In striking contrast, Lcn-2 levels in mice treated with DSS + GDNPs 2 were low and comparable to these in the water control group. These results suggest that GDNPs 2, but not GDNPs 1, exerted anti-inflammatory effects and were capable of preventing the intestinal inflammation induced by DSS. The anti-inflammatory effects of GDNPs 2 were further confirmed by the reduction in spleen weight (Fig. 3B); colon length also trended higher (Fig. 3C), although this difference did not reach statistical significance.

Mice were sacrificed 7 days after the start of treatments, and the histological effects of GDNPs on DSS-induced intestinal inflammation were examined by H&E staining. Mice treated with DSS water alone exhibited robust signs of inflammation, with epithelial erosion, interstitial edema, and a general increase in the number of inflammatory cells in the lamina propria (Fig. 3E). Interestingly, treatment with GDNPs 2, but not with GDNPs 1, prevented these signs of intestinal inflammation, particularly local lymphocytic infiltration, at the histological level. To confirm these initial observations, we measured colonic myeloperoxidase (MPO) activity as an indicator of the extent of neutrophil infiltration. As shown in Fig. 3D, the DSS-induced increase in MPO activity was indeed decreased significantly by GDNPs 2. In contrast, treatment with GDNPs 1 had no effect on DSS-induced MPO activity. Notably, oral administration of GDNPs 2 to untreated mice had no effect on cytokine levels or MPO activity, as noted in Fig. 5A.

E-cadherin plays a crucial role in epithelial cell-cell adhesion

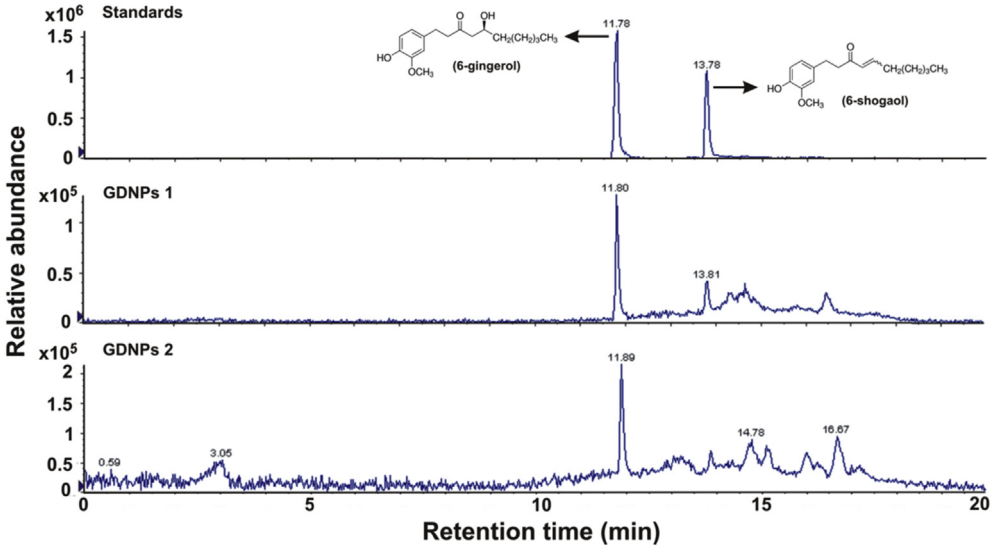

Fig. 2. Evaluation of the contents of 6-gingerol and 6-shogaol in ginger-derived nanoparticles (GDNPs) using HPLC/MS. Quantification of 6-gingerol and 6-shogaol in ginger derived nanopaticles, GDNPs 1 and GDNPs 2. The presence of GDNPs 1 and GDNPs 2 were confirmed by using standards and quantified using calibration curve for each individual component. (n = 3).

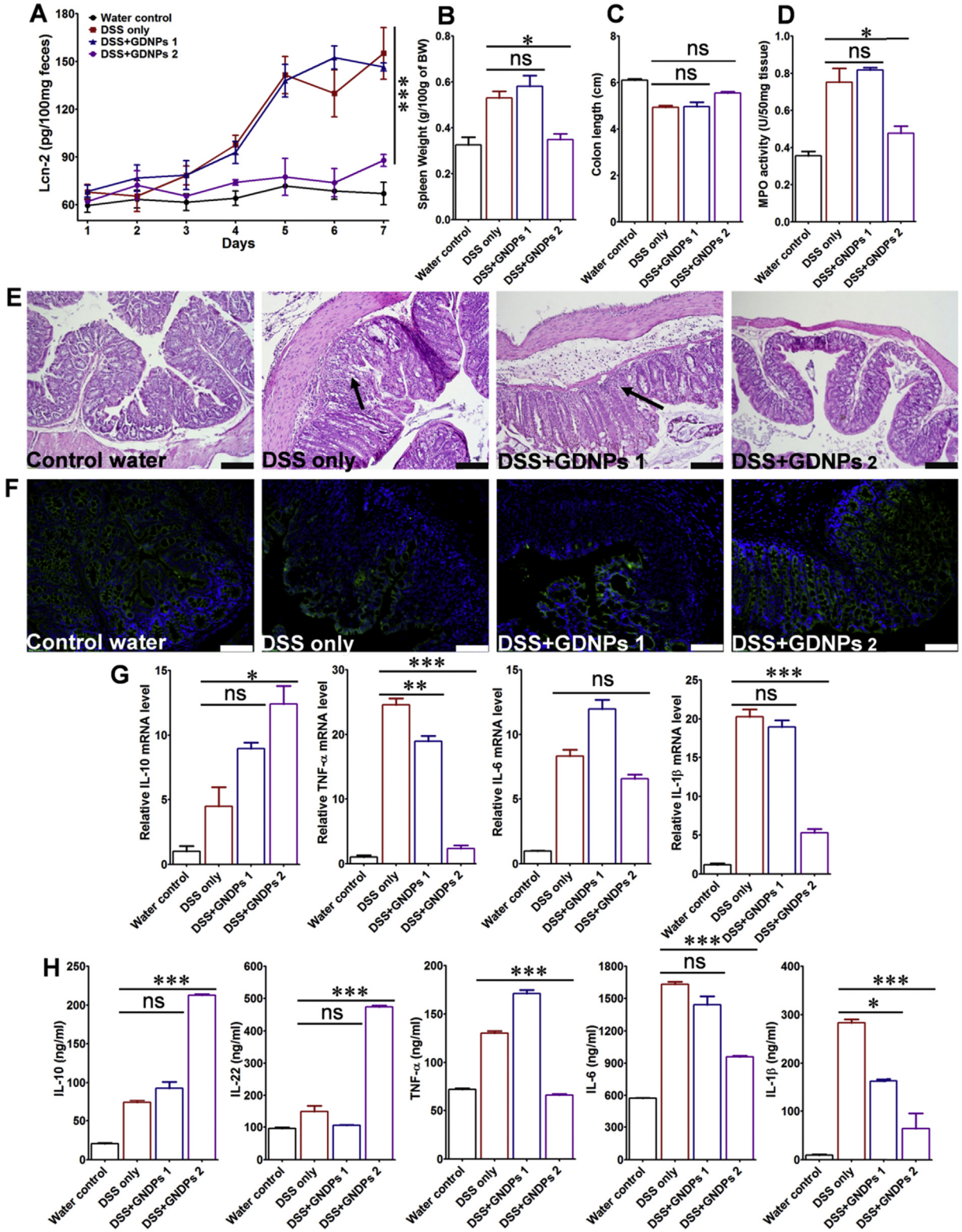

Fig. 3. The effect of orally administered GDNPs 2 on the susceptibility of mice to DSS-induced colitis. (A) Lcn-2 level. (B) Spleen/body weight. (C) Colon length. (D) Quantification of colonic MPO activity in the distal colon. (E) Representative H&E-stained colons. Inflammatory cells in the lamina propria are indicated by arrowheads. (F) Immunofluorescence staining for E-cadherin in representative inflamed areas of the colon. (G) Colonic levels of cytokine mRNAs were quantified by real-time RT-PCR and normalized with respect to the mRNA level of the ribosomal protein, 36B4. (H) Protein levels of colon-secreted cytokines were quantified by ELISA. For all panels: $^{*}p < 0.05$, $^{**}p < 0.01$, $^{***}p < 0.001$; ns, not significant; scale bar = 100 μm; n = 5.

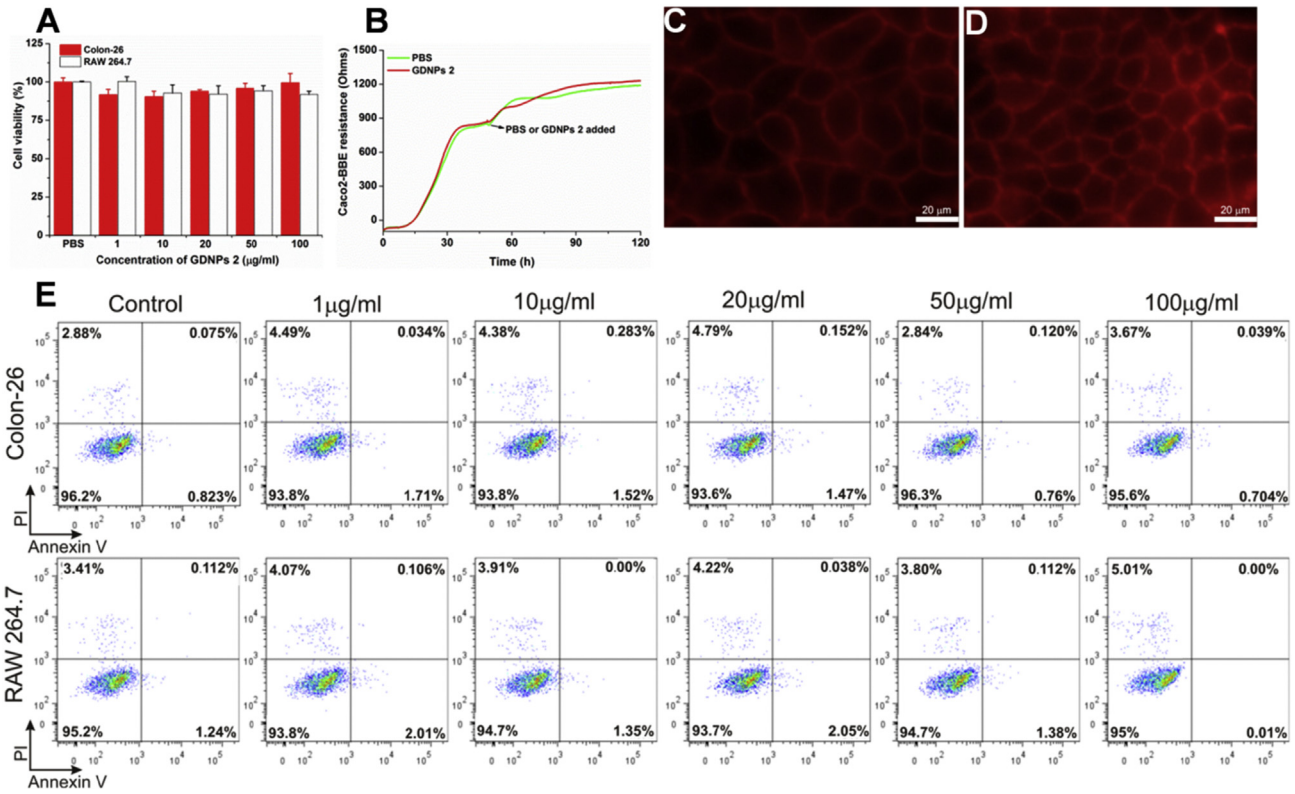

Fig. 4. Assess the biocompatibility of GDNPs *in vitro*. (A) MTT cell proliferation assay was used to assess the potential toxicity of GDNPs 2 in colon-26 and RAW 264.7 macrophage-like cell lines. (B) Barrier function assay was used to determine the influence of GDNPs 2 to the barrier function on caco2-BBE monolayer. (C) At the end of barrier function assay, PBS treated cells were stained with phalloidin-TRITC. Scale Bar = 20 μm. (D) At the end of barrier function assay, GDNPs 2 (100 μg/mL) treated cells were stained with phalloidin-TRITC. Scale Bar = 20 μm. (E) Cytotoxicity effect of GDNPs 2 on colon-26 cells and RAW 264.7 mouse macrophages after 24 h incubation were measured by FACS. Colon-26 and RAW 264.7 cells were incubated with indicated concentrations of GDNPs 2 for 24 h and then stained with Annexin-V/PI to detect the cell death. Lower left, viable cells (Annexin-V^-/PI^-); lower right, early apoptotic cells (Annexin-V^+/PI^-); upper left, necrotic cells (Annexin-V^-/PI^+); upper right, late apoptotic cells (Annexin-V^+/PI^+). (n = 3).

and in maintenance of tissue architecture. Down-regulation of E-cadherin expression is correlated with strong invasive potential; therefore, impaired expression of E-cadherin has been linked to disturbed intestinal barrier function and homeostasis [40–42]. An immunofluorescence analysis of different treatment regimens revealed that E-cadherin expression on colonic epithelial cells was dramatically increased in GDNPs 2 treated mice, but not in mice treated with GDNPs 1, compared with mice administered DSS water alone (Fig. 3F). These results corroborate the results of H&E staining (Fig. 3E).

3.6. Oral administration of GDNPs 2 does not affect cell viability or induce local or systemic side effects

In order to analyze potential toxicity, we first investigated the effects of GDNPs 1 and GDNPs 2 on colon-26 epithelial-like and RAW 264.7 macrophage-like cell lines *in vitro* using the MTT cell proliferation assay. As shown in Fig. 4A, treatment with GDNPs 2 for 24 h did not alter the viability of colon-26 and RAW 264.7 cells at any of the tested concentration of GDNPs 2 tested (up to 100 μg/ml). Electric cell-substrate impedance sensing (ECIS), which assesses the integrity of the intestinal barrier, was then used as a real-time method for testing toxicity [43]. Caco2-BBE cells were grown on transwell filters, and after the resistance had reached a plateau, PBS or GDNPs 2 (100 μg/mL) was added (Fig. 4B-D). GDNPs 2 did not affect the integrity of the barrier function of Caco2-BBE monolayers. Annexin/propidium iodide (PI) assays, which provide an indication of apoptosis/necrosis, revealed that GDNPs 2 at concentrations up to 100 μg/mL did not increase the percentage of apoptotic colon-26 or RAW 264.7 cells (Fig. 4E). Next, to evaluate the possible *in vivo* cytotoxicity of GDNPs 2, we administered GDNPs 2 (0.3 mg/mouse) daily to healthy mice by gavage for 7 days and quantitatively assessed colonic MPO activity and pro-inflammatory cytokines. There were no significant changes in MPO activity compared with controls (Fig. 5A), indicating the absence of neutrophil infiltration in GDNPs 2-treated colonic tissue. GDNPs 2 treatment also did not induce pro-inflammatory cytokines (TNF-α, IL-6 and IL-1β) at the mRNA or protein level (Fig. 5B, C). Moreover, a comparative analysis showed no differences in H&E staining, intestinal epithelial cell (IEC) proliferation, or IEC apoptosis in colonic tissues between groups (Fig. 5D). A histological examination of H&E-stained heart, liver, spleen, kidney, and lung showed no morphological or pathological changes in the GDNPs 2-gavaged group compared with controls (Supplementary Fig. 5). Taken together, these data suggest that orally administered GDNPs 2 do not cause toxicity or side effects at the local or systemic level. Notably, similar results were obtained with GDNPs 1 (data not shown).

3.7. Oral administration of GDNPs 2 blocks damaging factors while promoting pro-healing factors

The expression of pro-inflammatory cytokines is known to be involved in intestinal inflammation [44,45]. As expected, real-time RT-PCR experiments showed that DSS treatment increased the mRNA levels of the pro-inflammatory cytokines, TNF-α, IL-6, IL-1β, and decreased anti-inflammatory cytokine, IL-10 (Fig. 3G). Treatment with GDNPs 2, but not GDNPs 1, dramatically decreased the

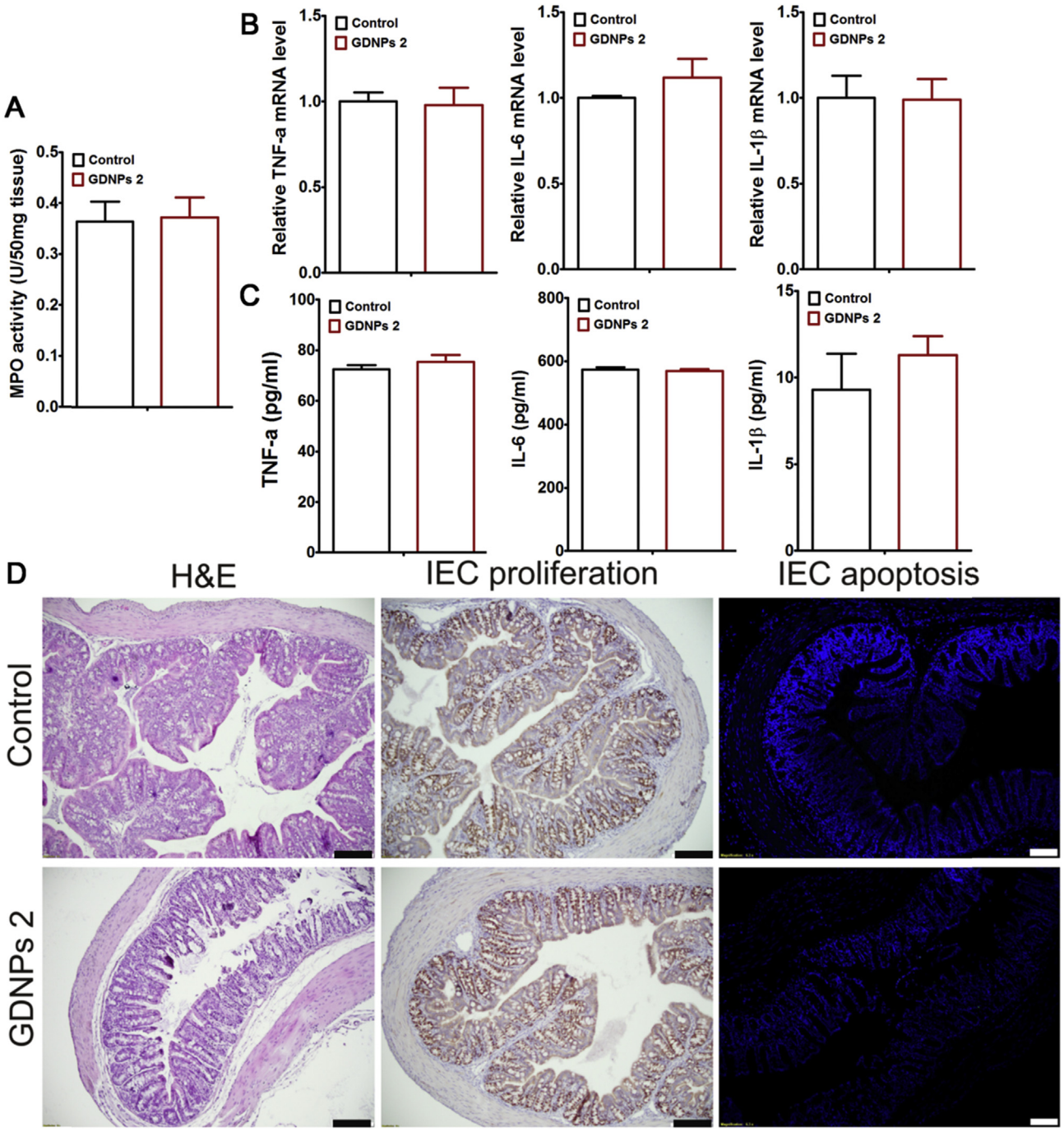

Fig. 5. Oral administration of GDNPs does not induce side effects at the local or systemic level. Mice (N = 5) were oral administrated with GDNPs 2 of 0.3 mg/day for 7 days. (A) Colonic myeloperoxidase (MPO) activity. (B) Quantify proinflammatory cytokines (TNF-α, IL-6 and IL-1β) at mRNA level. (C) Quantify proinflammatory cytokines (TNF-α, IL-6 and IL-1β) at protein level. (D) H&E stain, IEC proliferation and IEC apoptosis examination in colonic tissues. Scale Bar = 100 μm. (n = 5).

levels of tested pro-inflammatory cytokines, while increasing the levels of the tested anti-inflammatory cytokine IL-10. To assess the local protein levels of these pro- and anti-inflammatory cytokines, we generated colon cultures from mice of different treatment groups, as described in Materials and Methods. As shown in Fig. 3H, the protein levels obtained in these experiments were consistent with those of mRNA-based experiments, showing that treatment with GDNPs 2, but not with GDNPs 1, decreased the DSS-induced colonic secretion of pro-inflammatory cytokines and increased secretion of the anti-inflammatory cytokine IL-10 as well as that of IL-22. Taken together, these data demonstrate that the specific GDNPs 2 population of GDNPs confers anti-inflammatory effects against DSS-induced colitis by blocking the production of damaging pro-inflammatory cytokines, while enhancing the production of pro-healing anti-inflammatory cytokines, such as IL-10 and IL-22.

3.8. GDNPs 2 increase the survival and proliferation of IECs in DSS-induced colitis

The balance between apoptosis and cell proliferation determines normal tissue homeostasis. A key feature of intestinal homeostasis is the ability to maintain epithelial integrity and

trigger repair mechanisms following injury [46–48]. Based on our observation that GDNPs 2 decreased intestinal inflammation in DSS-induced colitis, we speculated that this population of GDNPs might decrease IEC apoptosis and increase IEC proliferation in response to DSS-induced injury. Accordingly, we assessed IEC apoptosis and proliferation in colonic sections using TUNEL (terminal deoxynucleotidyl transferase dUTP nick end labeling) assays and by staining for the proliferation marker Ki67, respectively (Supplementary Fig. 6). IEC apoptosis was increased and IEC proliferation was decreased in DSS-treated mice compared with water controls. In DSS-treated mice, administration of GDNPs 2, not but GDNPs 1, reduced IEC apoptosis while increasing IEC proliferation compared with that in mice that received DSS. Indeed, the levels of IEC proliferation in GDNPs 2-treated DSS mice and control mice that only received water were comparable. These results indicate that GDNPs 2 modulate the balance of apoptosis and cell proliferation during DSS-induced intestinal inflammation, thereby re-establishing tissue homeostasis.

3.9. Identification of molecular target candidates of GDNPs 2 involved in reducing colitis

Two-dimensional difference in-gel electrophoresis (2D-DIGE), with its high sensitivity and accuracy, has been a major tool for the identification of proteins [49,50]. To identify potential molecular targets of GDNPs 2 involved in reducing colitis, we used 2D-DIGE in conjunction with MS to analyze differential protein expression in colonic tissues from DSS-only mice and GDNPs 2-treated DSS mice. Proteins from the DSS-only group and GDNPs 2-treated DSS group were labeled with Cy5 (red) and Cy3 (green), respectively, for 2D-DIGE analysis; representative 2D-DIGE gel images are shown in Supplementary Fig. 7A. We identified a total of 24 spots that showed a change in intensity (defined as a DSS/GDNPs 2 vs DSS volume ratio $\geq$ 2). We then analyzed the proteins by MS and searched the raw data against the most recent FASTA databases for *Mouse* from Uniprot; the predicted protein names are presented. As shown in Supplementary Fig. 7B, 8 proteins were down-regulated and 16 proteins were up-regulated. Thus, these proteins are potentially involved in the anti-inflammatory activities of GDNPs 2 that reduce DSS-induced colitis.

3.10. Orally administered GDNPs 2 targets the colon and are taken up by epithelial cells and macrophages in mice with or without colitis

To confirm which cell population(s) of the colon takes up GDNPs 2 following oral administration, we isolated colonic epithelial cells and immune cells from both normal and DSS-treated mice 12 h after oral administration of GDNPs 2, and then performed flow cytometry. As shown in Fig. 6A-D, in normal mice 9.93% (Fig. 6A; Normal colon) of tested colonic epithelial cells ($EpCAM^+$) and 10.1% (Fig. 6D; Normal colon) of tested colonic macrophages cells ($CD11b^+F4/80^+$) had taken up GDNPs 2. In DSS-treated mice, by 9.89% (Fig. 6A, DSS colon) of tested colonic epithelial cells ($EpCAM^+$) and 11.6% (Fig. 6D, DSS colon) of tested colonic macrophage cells ($CD11b^+F4/80^+$) had taken up GDNPs 2. A small percentage of examined dendritic cells ($CD11c^+$) also showed uptake of GDNPs 2 in both normal (1.07%; Fig. 6B, Normal) and DSS-treated (1.24%; Fig. 6B, DSS) mice. GDNPs 2 were also efficiently taken up by colon-26 epithelial-like cells (Fig. 7A, B) and RAW 264.7 macrophage-like cells (Fig. 7C, D) in our *in vitro* experiments. Collectively, these results indicate that orally administered GDNPs 2 target the colon and further show that GDNPs are efficiently taken up by epithelial cells and macrophages in mice with or without colitis.

3.11. GDNPs 2 as therapeutics for colitis

Enhancement of intestinal repair mechanisms by modulatory factors may form the basis of future approaches for the treatment of diseases characterized by injuries of the epithelial surface [51,52]. Having confirmed that GDNPs 2 can ameliorate colitis symptoms in DSS-induced inflammation, we further speculated that GDNPs 2 might be able to increase healing of the inflamed mucosa in induced colitis. To test this, we first investigated the effects of GDNPs 2 on wound healing *in vitro* using ECIS technology. This device takes AC impedance measurements using weak and noninvasive AC signals, as previously described [53]. We first determined the ideal frequency for measuring the resistance of confluent Caco2-BBE monolayers. Monolayers grown on ECIS 8W1E plates were wounded by subjecting them to a 30-s pulse with a frequency of 40 kHz and amplitude of 4.5 V. ECIS measurements revealed that wounded epithelia cultured in the presence of GDNPs 2 (500 μl of a 0.1 mg/ml solution) healed significantly faster than PBS (500 μl)-treated controls (Fig. 8A). These data suggest that GDNPs 2 enhance the wound-healing process in epithelia. In contrast, DC-Chol/DOPE liposomes (Supplementary Fig. 8), considered among the most efficient vectors for introduction into cells *in vitro* and in clinical trials [54], reduced wound healing of intestinal epithelial cells at concentrations similar to those of GDNPs 2. Thus, our experiments demonstrate the feasibility of generating "natural" nanovectors assembled from ginger nanoparticle-derived lipids that mediate efficient *in vivo* drug delivery and exert no cytotoxicity or untoward effects on intestinal barrier function.

To extend our *in vitro* observations showing that GDNPs 2 may be beneficial for mucosal healing, we performed *in vivo* experiments. Mice were provided drinking water containing 1.5% DSS for 7 days (wounding phase), after which they were provided water alone or water plus a once-daily dose of GDNPs 2 (300 μl of a 1 mg/ml solution) administered by gavage for an additional 7 days (healing phase). Control mice, which had access to water alone, showed a slight increase in body weight (Fig. 8B), but no increase in measured levels of Lcn-2 (Fig. 8C), a marker used for the non-invasive assessment of colitis development [55]. DSS wounded mice maintained their body weights during the 7-day course of DSS administration, but their Lcn-2 levels increased during this period. After replacing DSS water with water alone (Fig. 8B, C, green dots), mice lost up to 20% of their body weight and showed an increase in Lcn-2 until day 11. By Day 14, mice had not recovered their initial (before DSS treatment) body weight and displayed high levels of Lcn-2, indicative of active intestinal inflammation. In contrast, mice gavaged once daily with GDNPs 2 lost significantly less body weight and had lower levels of Lcn-2 at Day 11 compared with control mice. In addition, mice treated with GDNPs 2 almost completely recovered their pretreatment body weights and Lcn-2 levels by Day 14. Similarly, a histological analysis (Fig. 8E) and an assessment of colonic MPO activity (Fig. 8D) also confirmed decreased intestinal mucosal ulceration and the extent of neutrophil infiltration in mice treated with GDNPs 2. mRNA for the pro-inflammatory cytokines, TNF-α, IL-1β and IL-6, and the anti-inflammatory cytokine IL-10 were highly expressed in the recovery group (DSS water) compared with that in the GDNPs 2-treated group (Fig. 9A). An analysis of pro- and anti-inflammatory cytokine protein levels yielded results that were consistent with those of mRNA-based experiments, showing that GDNPs 2 decreased the secretion of pro-inflammatory cytokines TNF-α, IL-6 and IL-1β, and increased the secretion of corresponding anti-inflammatory cytokines IL-10 and IL-22, changes that likely account for the accelerated healing of intestinal mucosal injuries and recovery of cytokines levels to normal in GDNPs 2-treated mice (Fig. 9B). Ki67 staining and TUNEL

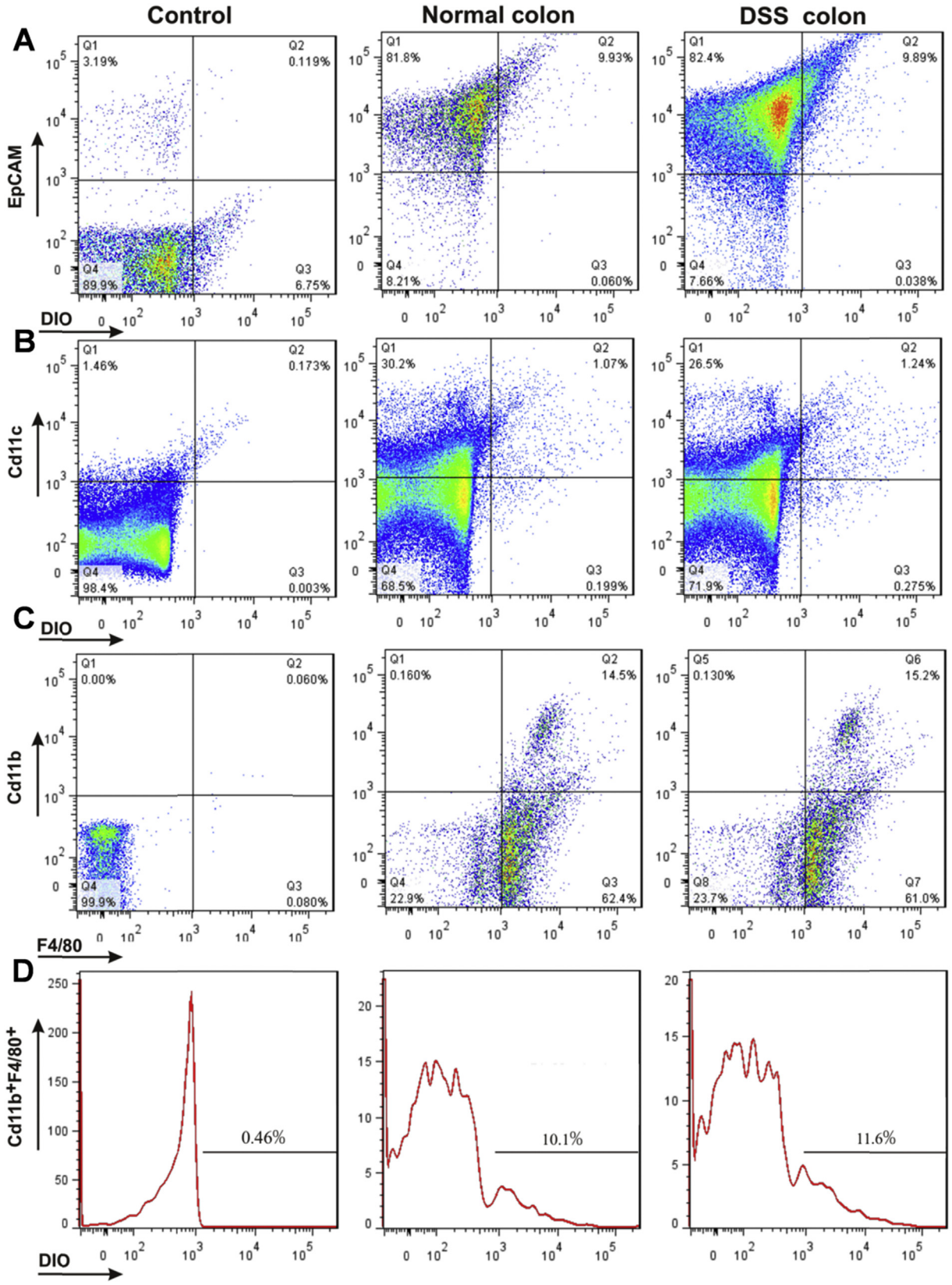

Fig. 6. Quantification of uptake efficiency of GDNPs 2 by epithelial cells and macrophages *in vivo* using flow cytometry. (A) Colonic epithelial cells ($EpCAM^+$), isolated and gated based on EpCAM. (B) Dendritic cells ($CD11c^+$), gated based on CD11c. (C) Macrophages ($CD11b^+F4/80^+$), gated based on CD11b and F4/80. (D) DiO-positive cells among $Cd11b^+F4/80^+$ macrophages. For control, epithelial cells ($EpCAM^+$), dendritic cells ($CD11c^+$) and macrophages ($CD11b^+F4/80^+$) cells were isolated from normal mice without GDNPs 2 oral administration using the same method. (n = 3).

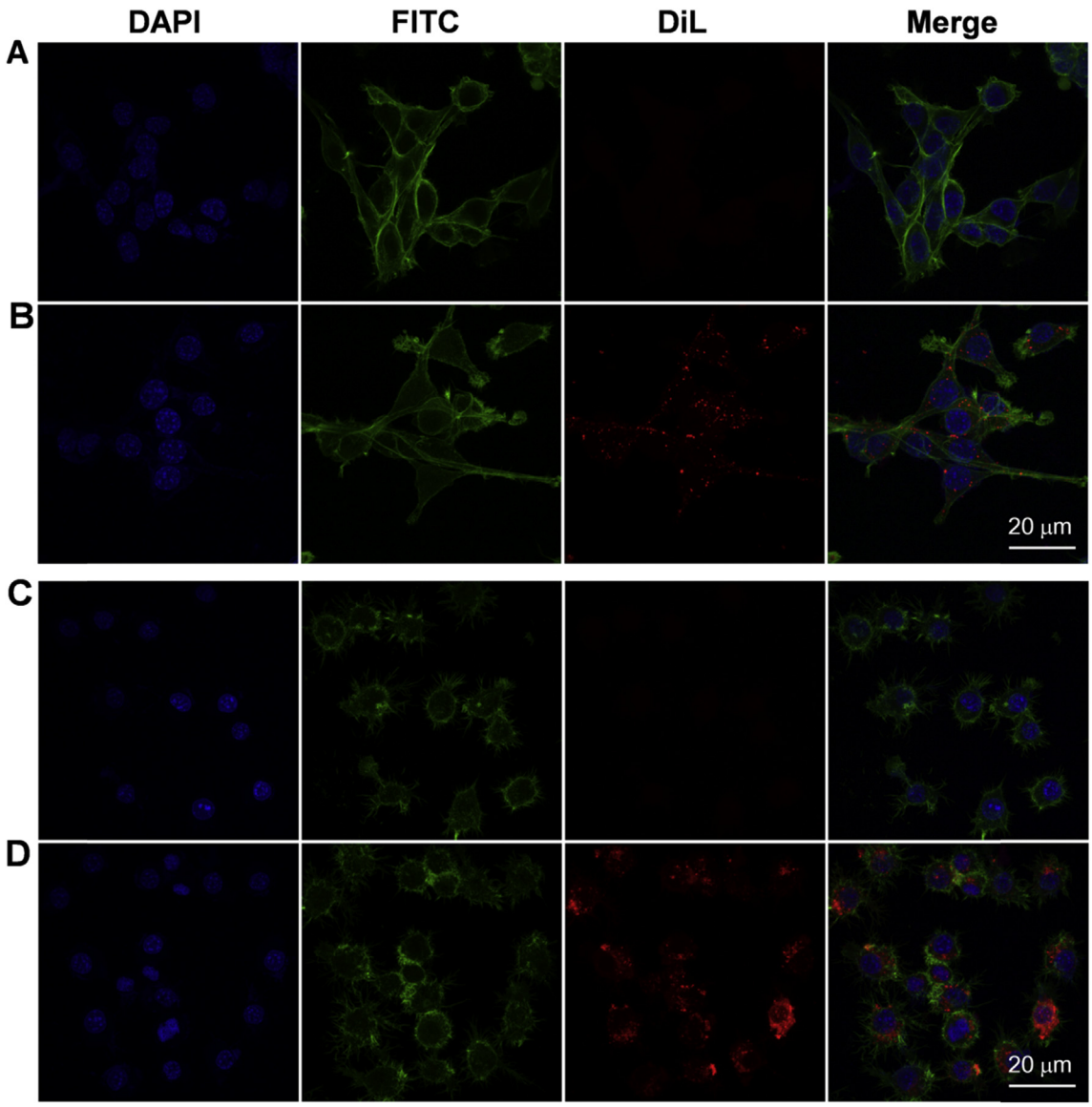

Fig. 7. The uptake of GDNPs 2 by epithelial-like (colon-26) and macrophage-like (macrophage 264.7) cells *in vitro*. (A) Colon-26 cells labeled with DAPI (blue channel) and phalloidin-FITC (green channel). (B) Colon-26 cells incubated with DiL-GDNPs 2 and then labeled with DAPI and phalloidin-FITC. (C) Macrophage cells labeled with DAPI and phalloidin-FITC. (D) Macrophage cells incubated with DiL-GDNPs 2 and then labeled with DAPI and phalloidin-FITC. (For interpretation of the references to colour in this figure legend, the reader is referred to the web version of this article.)

assays also confirmed that GDNPs 2 promoted intestinal mucosal healing (Supplementary Fig. 9).

3.12. Identification of molecular target candidates of GDNPs 2 involved in promoting intestinal mucosal healing

To identify potential molecular targets of GDNPs 2 involved in mucosal healing colitis, we used 2D-DIGE and MS to analyze proteins in colonic tissues that were differentially expressed between mice in the DSS-only group and GDNPs 2-treated DSS group. Both groups were administered DSS for 7 days (wounding phase); during the next 7 days (healing phase), mice in the DSS-only group received water and mice in the GDNP2-treatment group received water and a once-daily dose of GDNPs 2. Mice were sacrificed at the end of the healing phase and colonic proteins were isolated. Proteins from DSS-only group and GDNPs 2-treated DSS group were labeled with Cy5 (red) and Cy3 (green), respectively, for 2D-DIGE analysis. Representative 2D-DIGE gel images are shown in Supplementary Fig. 10A. We identified a total of 19 spots that showed a change in intensity (defined as a DSS/GDNPs 2 DSS volume ratio $\geq$ 5) between the DSS-only group and the GDNPs 2-treated DSS group. We then analyzed proteins by MS and searched the raw data against the most recent FASTA databases for *Mouse* from Uniprot; the predicted protein names, molecular weights, PI and peptide counts are presented in Supplementary Fig. 10B, which shows that 10 proteins were down-regulated and 9 were up-regulated in colonic tissue from GDNPs 2-treated DSS mice compared with tissue from mice in the DSS-only group. These proteins are potentially involved in the intestinal mucosal healing activities of GDNPs 2.

3.13. Treatment with GDNPs 2 prevents chronic colitis

To assess the anti-inflammatory effects of GDNPs 2 in a chronic colitis model, we chose IL-10 knockout ($IL10^{-/-}$) mice, which develop colitis with histopathological features that closely

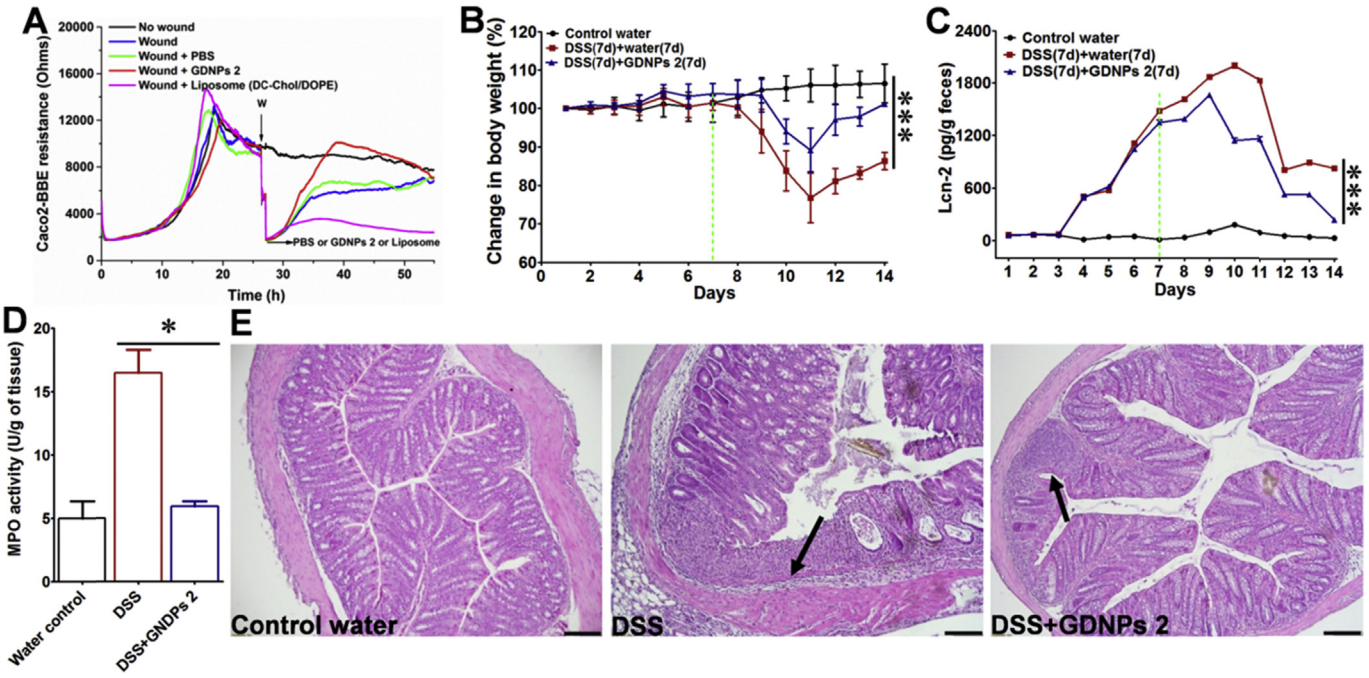

Fig. 8. Effect of GDNPs 2 in *in vitro* and *in vivo* wound-healing models. (A) GDNPs 2 accelerate healing in wounded intestinal epithelial monolayers using ECIS technology. (B) Body weight changes. (C) Lcn-2 changes. (D) MPO activity changes. (E) H&E-staining. Inflammatory cells in the lamina propria are indicated by arrowheads. Scale bar = 100 μm. (n = 5).

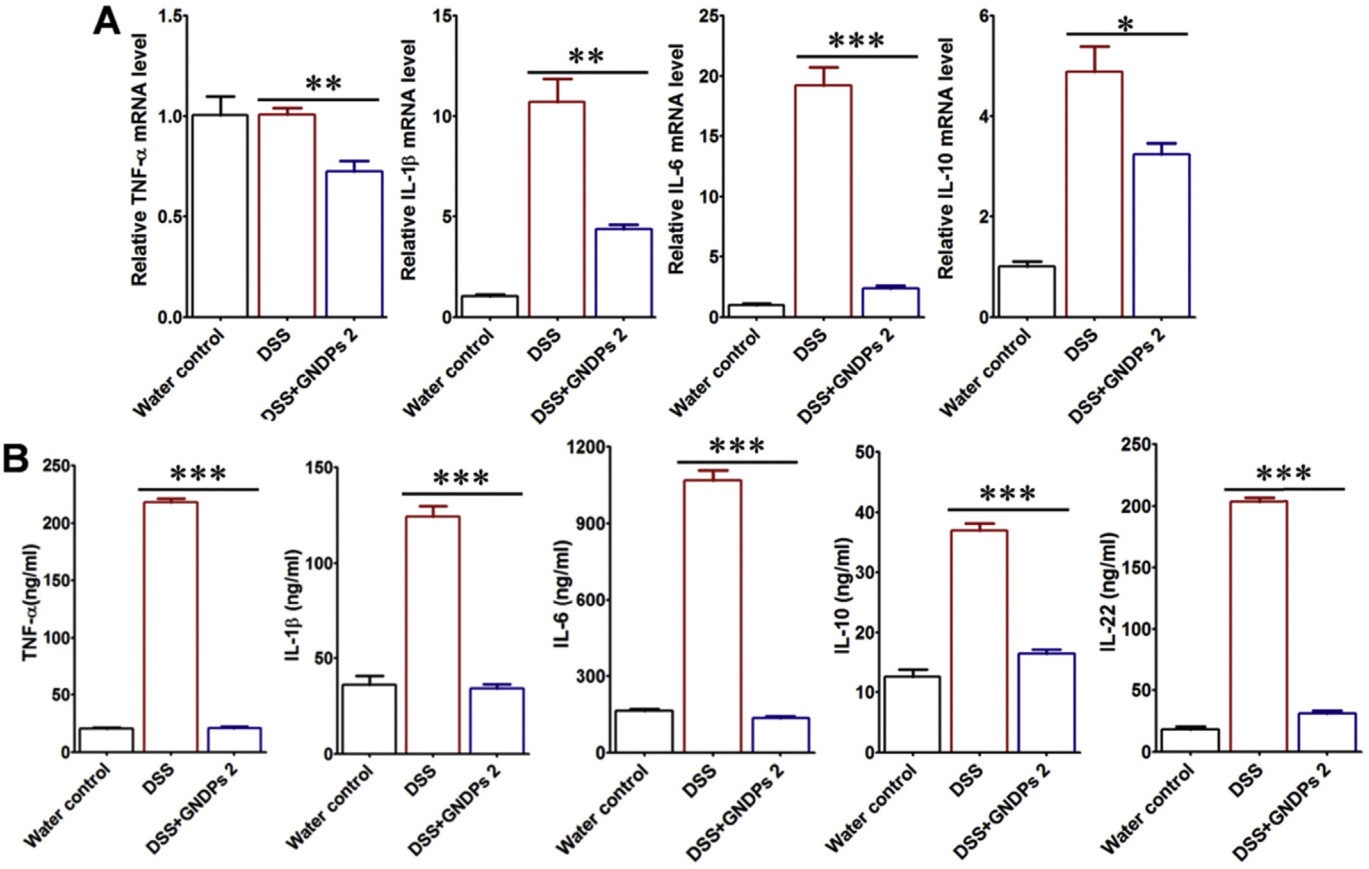

Fig. 9. Measurement of mRNA and protein levels of various cytokines in the DSS-induced mouse model of wound healing. (A) Cytokine mRNAs were quantified by real-time PCR. **(B)** Cytokines proteins were quantified by ELISA kits. $^{*}p < 0.05$, $^{**}p < 0.01$, $^{***}p < 0.001$. (n = 5).

recapitulate IBD [56,57]. In our facilities, IL10$^{-/-}$ mice spontaneously develop colitis in a time-dependent manner, exhibiting fully developed colitis within 18 weeks post weaning [58]. One group of IL10$^{-/-}$ mice were fed normally for 18 weeks after weaning, and a second group received orally administered GDNPs 2 (300 μl of 1 mg/ml solution) once daily for 18 weeks. At the end of the experiment (18 weeks after weaning), both groups of mice were sacrificed and the effects of GDNPs 2 were assessed. We observed that treatment with GDNPs 2 slightly decreased spleen weight (Fig. 10A) and increased colon length compared with IL10$^{-/-}$ mice not treated with GDNPs 2 (Fig. 10B). We also observed that GDNPs 2 treatment reduced colonic MPO levels compared with that in untreated IL10$^{-/-}$ mice, indicating diminished neutrophil infiltration in the GDNPs 2-treated group (Fig. 10C). Anti-inflammatory effects of GDNPs 2 were also confirmed based on histological features in H&E-stained samples. Untreated IL10$^{-/-}$ mice displayed obvious signs of inflammation, with immune cell infiltration and epithelial erosion at 12 weeks of age and more significant signs of inflammation at 22 weeks (Fig. 10D). In contrast, signs of mucosal inflammation in GDNPs 2-treated IL10$^{-/-}$ mice at 12 and 22 weeks post weaning were significantly reduced (Fig. 8D). We further showed that treatment with GDNPs 2 significantly decreased the expression of colonic pro-inflammatory cytokines (TNF-α, IL-1β) (Fig. 10E), confirming the anti-inflammatory effects of GDNPs 2 in the development of spontaneous colitis. Notably, the pro-inflammatory cytokine IL-6 was only slightly decreased in GDNPs 2-treated IL10$^{-/-}$ mice compared with untreated IL10$^{-/-}$ mice (Fig. 10E). Together, these results demonstrate that GDNPs 2 possess anti-inflammatory activity in a mouse model of chronic colitis.

3.14. Treatment with GDNPs 2 prevents CAC

A common complication of ulcerative colitis is colitis-associated cancer. Among the chemically induced colorectal cancer (CRC) models, the combination of a single “hit” of azoxymethane (AOM; 10 mg/kg body weight) with two, 1-week cycles of 2% DSS exposure in rodents recapitulates the aberrant crypt foci-adenoma-carcinoma sequence that occurs in human CRC [59,60]. Using this AOM model, we left one group of mice untreated (AOM/DSS) while treating another group of mice (AOM/DSS-GDNPs 2) by orally administering GDNPs 2 (0.3 mg) daily throughout the experiment by gavage (Fig. 11A). Although treatment with GDNPs 2 did not significantly change body weight compared with mice in the untreated AOM/DSS group (Supplementary Fig. 11A), it significantly reduced the inflammation level in the AOM/DSS-GDNPs 2 treatment group, as measured by the level of Lcn-2 (Supplementary Fig. 11B). AOM/DSS mice developed tumors from the middle to the distal portion of the colon (Fig. 11B) [44]. Both tumor numbers per mouse and tumor loads were significantly decreased by GDNPs 2 treatment of AOM/DSS mice (Fig. 11B). Specifically, treatment with GDNPs 2 decreased the number of tumors larger than 3 mm in size (although not the average tumor size) compared with untreated DSS/AOM mice. Importantly, treatment of AOM/DSS mice with GDNPs 2 reduced colonic MPO activity compared with untreated AOM/DSS mice (Fig. 11C). Moreover, an assessment of the effect of GDNPs 2 treatment on pro-inflammatory cytokine production in AOM/DSS mice revealed that the pro-inflammatory cytokines IL-6 and IL-1β were significantly decreased in the GDNPs 2-treatment group compared with the AOM/DSS group. Treatment with GDNPs 2 also produced a trend of decreased levels of TNF-α, although this difference failed to reach statistical significance owing to substantial inter-individual variability (Fig. 11C). In association with these changes, cyclin D1 mRNA levels were also decreased in the GDNPs 2-treatment group (Fig. 11C), suggesting that orally administered GDNPs 2 decrease cell proliferation during CAC development. Apoptosis also plays an important role in CAC, since greater apoptosis could induce cell proliferation to maintain homeostasis [61]. TUNEL assays showed that orally administered GDNPs 2 decreased apoptosis (Fig. 11D). Taken together, these data indicate that GDNPs 2 decrease colorectal tumorigenesis by reducing pro-inflammatory cytokine levels and inhibiting IEC proliferation and apoptosis. This further suggests that the ability of GDNPs 2 to reduce inflammation might be secondary to reductions in tumor development.

3.15. Identification of molecular target candidates of GDNPs 2 involved in reducing CAC

We also identified potential molecular targets of GDNPs 2 involved in reducing CAC using 2D-DIGE/MS. Proteins from the AOM/DSS group and the GDNPs 2-treated group were labeled with Cy5 (red) and Cy3 (green), respectively. Representative 2D-DIGE gel images are shown in Supplementary Fig. 12A. We identified a total of 17 spots that showed a change in intensity (defined as an AOM/DSS/GDNPs 2 vs AOM/DSS volume ratio ≥ 5). We then analyzed the proteins by MS and searched the raw data against the most recent FASTA databases for *Mouse* from Uniprot. The predicted protein names are presented in Supplementary Fig. 12B, which showed that 3 proteins were down-regulated and 14 proteins were up-regulated. These proteins are potentially involved in reducing colitis associated cancer.

4. Discussion

Targeting drug carriers based on nanoparticles have been designed and have shown great promise for improving IBD treatment. Various carriers have been designed to release the drug at a specific pH value, to be resistant to digestive enzymes, and/or require bacterial cleavage for activation, and several of these carriers are currently being investigated. The application of plants as “nanofactories” for the fabrication of medical nanoparticles could represent a new approach for IBD treatment. In this study, we isolated and identified three populations of nanoparticles—GDNPs 1, GDNPs 2 and GDNPs 3-from edible plant ginger. GDNPs 1 and GDNPs 2 exhibited a zeta potential values of approximately −2 to −12 mV at pH 6 (~colon pH), indicating mutual repulsion of nanoparticles with no tendency towards aggregation. The average size of GDNPs was ~220–290 nm. A monodispersed size distribution is considered an essential design criterion for an effective nanoparticle. The size distribution and zeta potential of GDNPs was in the range of other isolated edible nanoparticles from grape and grapefruit [29,30]. An analysis of GDNPs lipid profiles revealed predominantly phosphatidic acid, digalactosyldiacylglycerol and monogalactosyldiacyglycerol, which were present in roughly similar amounts in the different GDNPs populations. Notably, phosphatidic acid is highly fusogenic in the presence of calcium [62], and has been postulated to induce inter-vesicular fusion [63]. Interestingly, we found that the lipid profile of each GDNP population (GDNPs 1, GDNPs 2 and GDNPs 3) was similar to that of other edible nanoparticles from grapefruit and grape that have been previously isolated [29,30]. We further found that the protein content of GDNPs was low, and was primarily in the form of cytosolic proteins, with few membrane proteins, an observation in agreement with the protein profile reported for grape nanoparticles [29]. We also showed that GDNPs 2 contains 125 miRNAs (15–27 nucleotides in length) that were unique to GDNPs 2 compared with those reported in grape nanoparticles -all but one of which have the potential to regulate the expression of human genes by binding to their 3'-UTRs. Both 6-gingerol and 6-shogaol, two major anti-

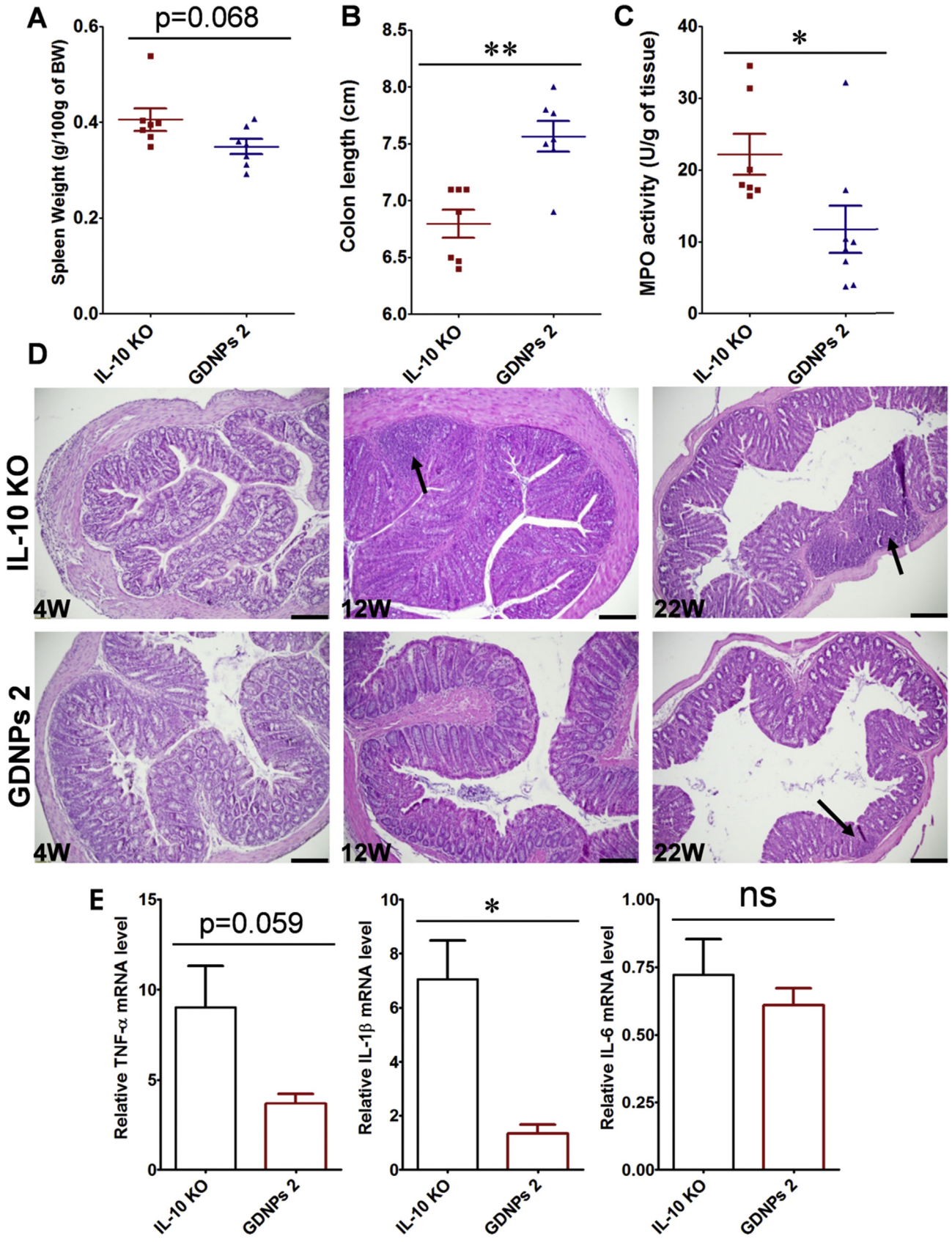

Fig. 10. Effect of GDNPs 2 on chronic colitis in IL10$^{-/-}$ mice. (A) Spleen/body weight. (B) Colon length. (C) MPO activity. (D) Representative H&E-stained colon sections. Inflammatory cells in the lamina propria are indicated by arrowheads. (E) Pro-inflammatory cytokines mRNAs were quantified by real-time RT-PCR. *$p < 0.05$, **$p < 0.01$, ***$p < 0.001$; ns, not significant. Scale bar = 100 μm. (n = 7).

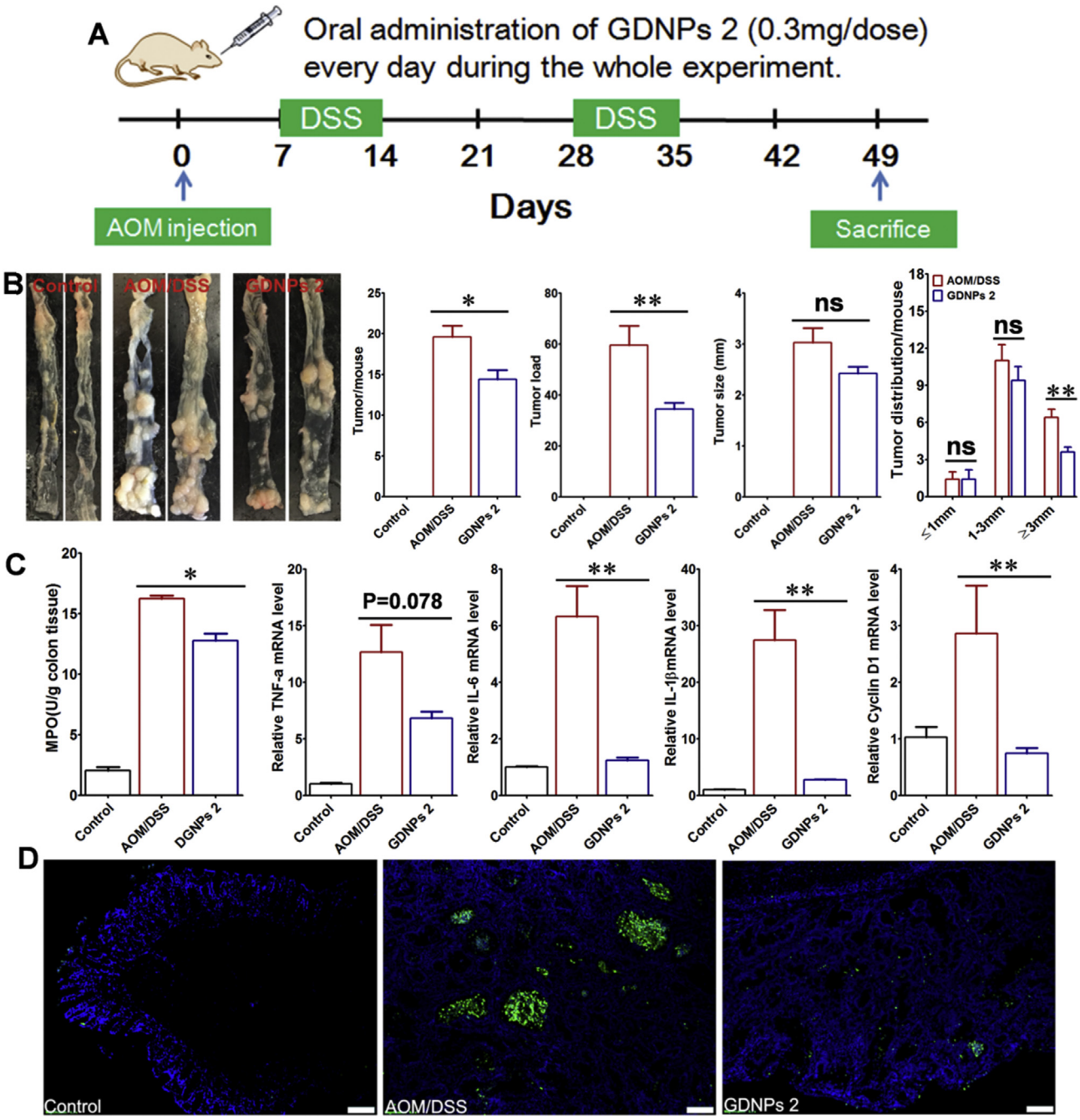

Fig. 11. Effect of GDNPs 2 on colitis-associated cancer (CAC). (A) Protocol for CAC induction. Mice were administered GDNPs 2 (0.3 mg/dose) daily in treatment group. (B) Colon tumor/mouse, tumor load, tumor size and tumor distribution were obtained at the end of the CAC protocol. (C) MPO activities mRNA levels of cytokines and cyclin D1 were quantified. (D) Apoptosis of cells was quantified by TUNEL assay (FITC, green color) and nuclei were stained with DAPI (blue). $^{*}p < 0.05$, $^{**}p < 0.01$, $^{***}p < 0.001$; ns, not significant. Scale bar = 100 μm. (n = 5). (For interpretation of the references to colour in this figure legend, the reader is referred to the web version of this article.)

inflammatory and anti-cancer compounds, are components of ginger [64–66]. Interestingly, we found that GDNPs 2 contained higher concentrations of these active ginger constituents compared with GDNPs 1 and GDNPs 3. In sum, our characterization revealed these three populations of GDNPs that consist of specific natural membrane lipids with a few membrane proteins, and contain miRNAs and different levels of 6-gingerol and 6-shogaol. Importantly, we found that 1000 g of ginger yielded ~50 mg of GDNPs (GDNPs 1, GDNPs 2 and GDNPs 3)—a high production yield of GDNPs compared with synthesized nanoparticles that highlights the potential for large-scale production of GDNPs. GDNPs 2, which showed the highest levels of active ginger compounds, and GDNPs 1, which, like GDNPs 2, were very stable at room temperature and tolerant of freeze/thaw cycles, were selected for further analysis in tests of anti-inflammatory activity in experimental colitis.

Unlike most IBD drugs, which must be administered systemically and are thus associated with serious side effects [67,68], GDNPs 2 are delivered orally, offering several advantages over other therapeutic routes. Importantly, oral administration supports our primary goal of delivering GDNPs 2 to the colon, which is the site of intestinal inflammation in ulcerative colitis. Our results indicate effective retention of orally administered GDNPs in the colon,

especially in non-starved mice. These results are in agreement with previous studies showing that orally administered grape nanoparticles are stable during transition through the stomach and small intestine, and target the colon. They are also important for the potential use of GDNPs 2 as a colon-targeting nanoparticle system. Notably, the targeted delivery of GDNPs 2 to the colon made possible by oral administration did not induce local or systemic side effects. Once GNDPs 2 reached the colon, they were taken up equally by IECs and macrophages in mice with or without colitis. This dual cellular targeting of orally administered GDNPs 2 is unique compared with nanoparticles from grape and grapefruit, which primarily target intestinal macrophages and intestinal stem cells (ISCs), respectively [29,30].

Comparative functional analyses of the two GDNPs populations that showed favorable biophysical properties (GDNPs 1 and GDNPs 2) revealed that orally administered GDNPs 2, but not GDNPs 1, reduced acute inflammation induced by DSS, suggesting that the higher content of 6-gingerol and 6-shogaol in GDNPs 2 might play a role in their anti-inflammatory activities. Interestingly, orally administered GDNPs 2 increased the survival and proliferation of IECs, reduced expression of the pro-inflammatory cytokines (TNF-α, IL-6 and IL-1β), and increased expression of the anti-inflammatory cytokines (IL-10 and IL-22) in induced colitis, suggesting that GDNPs 2 block factors that damage the intestines while promoting factors that heal them. An analysis of differentially expressed genes following oral administration of GDNPs also identified molecular targets of GDNPs 2 that are potentially involved in reducing acute colitis. Most of these molecular targets are proteins expressed in cell cytoplasm, membrane, mitochondria or nucleus of the intestinal mucosa. For example, GDNPs 2 increased expression of NRROS (negative regulator of reactive oxygen species), which is known to limit ROS production by phagocytes during the inflammatory response and thus “cools off” inflammation [69]. Accumulating evidence places mitochondria at the center of diverse cellular functions and suggest mitochondria as integrators of signaling pathways, such as inflammation [70]. In this context, it was not surprising that GDNPs 2 affected the expression of numerous mitochondrial proteins, including malate dehydrogenase, creatine kinase B-type, ATP synthase subunit beta, and succinate dehydrogenase. In acute colitis, intestinal barrier function is compromised by dysregulation of the cytoskeleton and junction proteins [71–73]. In our study, we found that GDNPs 2 affected the expression of numerous cytoskeleton proteins, including adseverin, cofillin-1, KRT19 (keratin, type I cytoskeletal 19), KRT78 (keratin 78 type II), and the adherens junction protein, desmoglein. We also found that nuclear proteins, such as ZMYND11 (zinc finger, MYND-type containing 11), were targeted by GDNPs 2.

Using *in vitro* and *in vivo* wound-healing models, we demonstrated that GDNPs 2 promote intestinal mucosa healing. Interestingly, treatment of wounded intestinal mucosal with GDNPs 2 reestablished normal levels of pro- and anti-inflammatory cytokines and MPO activity, and restored IEC proliferation-apoptosis balance in the intestinal mucosa. We further demonstrated that the molecular targets of GDNPs 2 at the end of the healing phase were primarily cytoplasmic/membrane proteins of the intestinal mucosa. For example, GDNPs 2 treatment dramatically increased the expression (~14-fold) of CAR1 (carbonic anhydrase 1), which is known to be present on the surface of enterocytes of the colon [74,75] and is a major cecal antigen that has been implicated in the pathogenesis of IBD [76]. Notably, oral tolerization with CAR1 is effective in the treatment of a murine model of IBD [77]. Treatment with GDNPs 2 also attenuated expression of the secreted protein hemopexin, a result that is in agreement with a previous report showing that hemopexin expression is related to the degree of intestinal injury [78]. We further found that GDNPs 2 affected the expression of mitochondrial proteins, such as HSPA13 (heat shock protein family A [Hsp70] member 13), and cytoplasmic proteins such as axin and kinesin, which are involved in cell proliferation/division, and proteins such as ADAM8, KRT19 (keratin, type I cytoskeletal 19), flotillin-1 and ILK (integrin-linked protein kinase), which are involved in cell-cell adhesion during intestinal inflammation. Nuclear proteins such as SNRPD3 (small nuclear ribonucleoprotein Sm D3) were also targeted. Taken together, our results demonstrate that GDNPs 2 target the expression of multiple proteins that are involved in increasing mucosal healing after injury and consequently suggest that GDNPs 2 may be useful for colitis treatment.

We further investigated the effectiveness of GDNPs 2 for treating chronic colitis and CAC. Using the IL10$^{-/-}$ mouse model of chronic colitis, we discovered that GDNPs 2 treatment prevented disease progression. Because GDNPs 2 were administered before the manifestation of colitis in this model, these results demonstrate that GDNPs 2 may be useful for preventing colitis. The known link between chronic intestinal inflammation and the development of CRC, among the most common malignancies [79–81], has given rise to the term “colitis-associated cancer” [82]. The development of CAC in patients suffering from ulcerative colitis is one of the best clinically characterized examples of an association between intestinal inflammation and carcinogenesis [83]. CRC is a major cause of excess morbidity and mortality in ulcerative colitis as well as Crohn's disease patients. In fact, CRC is observed in 13.5% of all patients with ulcerative colitis, a risk rate that is at least 2-fold greater than that of the population as a whole. Here, using a mouse CAC model that combined AOM-induced carcinogenesis and DSS-induced chronic inflammation, we showed that treatment with GDNPs 2 reduced colonic tumor incidence and growth by reducing inflammation-induced IEC proliferation, as shown by the decrease in the proliferation marker, cyclin D1, and the reduction in the production of pro-inflammatory cytokines/chemokines, including the critical regulators IL-6, IL-1β and TNF-α. Interestingly, we found that GDNPs 2 treatment targeted expression of multiple proteins that have been implicated in the development of CAC. For example, recent studies have demonstrated that signaling through cGMP is an important regulator of tissue homeostasis in the gastrointestinal tract, showing that activation of cGMP-dependent protein kinase inhibits TCF (T cell transcription factor) signaling in colon cancer cells by blocking β-catenin expression and activating FOXO4 (forkhead box O4) [84,85]. Interestingly, we found that treatment with GDNPs 2 increased the expression of PKG, an effect that may be responsible, at least in part, for the therapeutic efficacy of GDNPs 2. This interpretation is supported by reports showing that therapeutic activation of cGMP/PKG is a promising avenue for the prevention and treatment of colon cancer [85]. Other proteins that have been suggested to be involved in the development of CAC include the GTP-binding nuclear protein Ran and transgelin [86–88], the latter of which has been shown to be significantly down-regulated in human colon tumors compared with adjacent non-tumorous tissues [89]. Important in this context, we found that treatment with GDNPs 2 increased transgelin expression, which may be another contributor to the therapeutic efficacy of GDNPs 2.

5. Conclusions

This study represents proof of principle that a novel, natural, nontoxic delivery system is capable of targeting the inflamed intestinal mucosa, and blocking damaging factors while promoting healing factors. This system, exemplified by GDNPs 2, can easily be developed for large-scale production and may ultimately represent an effective therapeutic strategy for preventing and treating IBD and CAC.

Acknowledgments

This work was supported by grants from the Department of Veterans Affairs (BX002526) and the National Institutes of Health of Diabetes and Digestive and Kidney (RO1-DK-071594 to D.M). M. Zhang and E. Viennois are recipients of a Research Fellowship Award from the Crohn's & Colitis Foundation of America. D. Merlin is a recipient of a Research Career Scientist Award from the Department of Veterans Affairs.

Appendix A. Supplementary data

Supplementary data related to this article can be found at http://dx.doi.org/10.1016/j.biomaterials.2016.06.018.

References

[1] J. Terzic, S. Grivennikov, E. Karin, M. Karin, Inflammation and colon cancer, Gastroenterology 138 (2010) 2101–2114.
[2] A.T. Chan, E.L. Giovannucci, Primary prevention of colorectal cancer, Gastroenterology 138 (2010) 2029–2043.
[3] D.A. Sussman, R. Santaolalla, S. Strobel, R. Dheer, M.T. Abreu, Cancer in inflammatory bowel disease: lessons from animal models, Curr. Opin. Gastroenterol. 28 (2012) 327–333.
[4] G.L. Stretch, B.J. Campbell, A.D. Dwarakanath, M. Yaqoob, A. Stevenson, A.I. Morris, et al., 5-Amino salicylic acid absorption and metabolism in ulcerative colitis patients receiving maintenance sulphasalazine, olsalazine or mesalazine, Aliment. Pharm. Ther. 10 (1996) 941–947.
[5] D. Pertuit, B. Moulari, T. Betz, A. Nadaradjane, D. Neumann, L. Ismaili, et al., 5-amino salicylic acid bound nanoparticles for the therapy of inflammatory bowel disease, J. Control Release 123 (2007) 211–218.
[6] S.B. Hanauer, New steroids for IBD: progress report, Gut 51 (2002) 182–183.
[7] U. Navaneethan, B.A. Lashner, Effects of immunosuppression and liver transplantation on inflammatory bowel disease in patients with primary sclerosing cholangitis, Clin. Gastroenterol. Hepatol. 11 (2013) 524–525.
[8] D.Z. Wang, R.N. DuBois, The role of anti-inflammatory drugs in colorectal cancer, Annu. Rev. Med. 64 (2013) 131–144.
[9] L.M. Ensign, R. Cone, J. Hanes, Oral drug delivery with polymeric nanoparticles: the gastrointestinal mucus barriers, Adv. Drug Deliv. Rev. 64 (2012) 557–570.
[10] S.F. Zhang, J. Ermann, M.D. Succi, A. Zhou, M.J. Hamilton, B.N. Cao, et al., An inflammation-targeting hydrogel for local drug delivery in inflammatory bowel disease, Sci. Transl. Med. 7 (2015) 300ra128.
[11] B. Xiao, H. Laroui, E. Viennois, S. Ayyadurai, M.A. Charania, Y.C. Zhang, et al., Nanoparticles with surface antibody against CD98 and carrying CD98 small interfering RNA reduce colitis in mice, Gastroenterology 146 (2014) 1289–1300.
[12] P.S. Dulai, C.A. Siegel, J.F. Colombel, W.J. Sandborn, L. Peyrin-Biroulet, Systematic review: monotherapy with antitumour necrosis factor alpha agents versus combination therapy with an immunosuppressive for IBD, Gut 63 (2014) 1843–1853.
[13] C. Moriasi, D. Subramaniam, S. Awasthi, S. Ramalingam, S. Anant, Prevention of colitis-associated cancer: natural compounds that target the IL-6 soluble receptor, Anti-Cancer Agent Med. Chem. 12 (2012) 1221–1238.
[14] M. Fukata, L.M. Shang, R. Santaolalla, J. Sotolongo, C. Pastorini, C. Espana, et al., Constitutive activation of epithelial TLR4 augments inflammatory responses to mucosal injury and drives colitis-associated tumorigenesis, Inflamm. Bowel Dis. 17 (2011) 1464–1473.
[15] X.H. Xing, B.B. Zhang, X.H. Wang, F.J. Liu, D.L. Shi, Y.S. Cheng, An "imaging-biopsy" strategy for colorectal tumor reconfirmation by multipurpose paramagnetic quantum dots, Biomaterials 48 (2015) 16–25.
[16] F. Araujo, N. Shrestha, M.A. Shahbazi, D.F. Liu, B. Herranz-Blanco, E.M. Makila, et al., Microfluidic assembly of a multifunctional tailorable composite system designed for site specific combined oral delivery of peptide drugs, ACS Nano 9 (2015) 8291–8302.
[17] A.E. Hansen, A.L. Petersen, J.R. Henriksen, B. Boerresen, P. Rasmussen, D.R. Elema, et al., Positron emission tomography based elucidation of the enhanced permeability and retention effect in dogs with cancer using Copper-64 liposomes, ACS Nano 9 (2015) 6985–6995.
[18] H. Laroui, G. Dalmasso, H.T.T. Nguyen, Y.T. Yan, S.V. Sitaraman, D. Merlin, Drug-loaded nanoparticles targeted to the colon with polysaccharide hydrogel reduce colitis in a mouse model, Gastroenterology 138 (2010) 843–853.
[19] S.C. Han, Q. Cheng, Y.D. Wu, J.H. Zhou, X.W. Long, T. Wei, et al., Effects of hydrophobic core components in amphiphilic PDMAEMA nanoparticles on siRNA delivery, Biomaterials 48 (2015) 45–55.
[20] B. Xiao, Y. Yang, E. Viennois, Y.C. Zhang, S. Ayyadurai, M.T. Baker, et al., Glycoprotein CD98 as a receptor for colitis-targeted delivery of nanoparticles, J. Mater Chem. B 2 (2014) 1499–1508.
[21] B. Xiao, H. Laroui, S. Ayyadurai, E. Viennois, M.A. Charania, Y.C. Zhang, et al., Mannosylated bioreducible nanoparticle-mediated macrophage-specific TNF-alpha RNA interference for IBD therapy, Biomaterials 34 (2013) 7471–7482.
[22] S. Ramishetti, R. Kedmi, M. Goldsmith, F. Leonard, A.G. Sprague, B. Godin, et al., Systemic gene silencing in primary T lymphocytes using targeted lipid nanoparticles, ACS Nano 9 (2015) 6706–6716.
[23] H. Laroui, A.L. Theiss, Y.T. Yan, G. Dalmasso, H.T.T. Nguyen, S.V. Sitaraman, et al., Functional TNF alpha gene silencing mediated by polyethyleneimine/TNF alpha siRNA nanocomplexes in inflamed colon, Biomaterials 32 (2011) 1218–1228.
[24] B. Xiao, X.Y. Si, M.Z. Zhang, D. Merlin, Oral administration of pH-sensitive curcumin-loaded microparticles for ulcerative colitis therapy, Colloid Surf. B 135 (2015) 379–385.
[25] L. Tang, R. Tong, V.J. Coyle, Q. Yin, H. Pondenis, L.B. Borst, et al., Targeting tumor vasculature with aptamer-functionalized doxorubicin - polylactide nanoconjugates for enhanced cancer therapy, ACS Nano 9 (2015) 5072–5081.
[26] S.W. Morton, M.J. Lee, Z.J. Deng, E.C. Dreaden, E. Siouve, K.E. Shopsowitz, et al., A nanoparticle-based combination chemotherapy delivery system for enhanced tumor killing by dynamic rewiring of signaling pathways, Sci. Signal 7 (2014) ra44.
[27] X.Y. Zhuang, Z.B. Deng, J.Y. Mu, L.F. Zhang, J. Yan, D. Miller, et al., Ginger-derived nanoparticles protect against alcohol-induced liver damage, J. Extracell. Vesicles 4 (2015) 28713.
[28] J.Y. Mu, X.Y. Zhuang, Q.L. Wang, H. Jiang, Z.B. Deng, B.M. Wang, et al., Interspecies communication between plant and mouse gut host cells through edible plant derived exosome-like nanoparticles, Mol. Nutr. Food Res. 58 (2014) 1561–1573.
[29] S.W. Ju, J.Y. Mu, T. Dokland, X.Y. Zhuang, Q.L. Wang, H. Jiang, et al., Grape exosome-like nanoparticles induce intestinal stem cells and protect mice from DSS-induced colitis, Mol. Ther. 21 (2013) 1345–1357.
[30] B.M. Wang, X.Y. Zhuang, Z.B. Deng, H. Jiang, J.Y. Mu, Q.L. Wang, et al., Targeted drug delivery to intestinal macrophages by bioactive nanovesicles released from grapefruit, Mol. Ther. 22 (2014) 522–534.
[31] M. Zhang, E. Viennois, C. Xu, D. Merlin, Plant derived edible nanoparticles as a new therapeutic approach against diseases, Tissue Barriers 4 (2016) e1134415.
[32] M. Brahmbhatt, S.R. Gundala, G. Asif, S.A. Shamsi, R. Aneja, Ginger phytochemicals exhibit synergy to inhibit prostate cancer cell proliferation, Nutr. Cancer 65 (2013) 263–272.
[33] P. Karna, S. Chagani, S.R. Gundala, P.C.G. Rida, G. Asif, V. Sharma, et al., Benefits of whole ginger extract in prostate cancer, Brit J. Nutr. 107 (2012) 473–484.
[34] M.S. Butt, M.T. Sultan, Ginger and its health claims: molecular aspects, Crit. Rev. Food Sci. 51 (2011) 383–393.
[35] S. Prasad, B.B. Aggarwal, Chronic diseases caused by chronic inflammation require chronic treatment: anti-inflammatory role of dietary spices, J. Clin. Cell Immunol. 2014 (2014).
[36] A.C. Brown, C. Shah, J. Liu, J.T.H. Pham, J.G. Zhang, M.R. Jadus, Ginger's (Zingiber officinale roscoe) inhibition of rat colonic adenocarcinoma cells proliferation and angiogenesis in vitro, Phytother. Res. 23 (2009) 640–645.
[37] R. Grzanna, L. Lindmark, C.G. Frondoza, Ginger - an herbal medicinal product with broad anti-inflammatory actions, J. Med. Food 8 (2005) 125–132.
[38] E.A. Al-Suhaimi, N.A. Al-Riziza, R.A. Al-Essa, Physiological and therapeutical roles of ginger and turmeric on endocrine functions, Am. J. Chin. Med. 39 (2011) 215–231.
[39] E. Viennois, B. Xiao, S. Ayyadurai, L.X. Wang, P.G. Wang, Q. Zhang, et al., Micheliolide, a new sesquiterpene lactone that inhibits intestinal inflammation and colitis-associated cancer, Lab. Invest. 94 (2014) 950–965.
[40] J.R. Turner, Intestinal mucosal barrier function in health and disease, Nat. Rev. Immunol. 9 (2009) 799–809.
[41] S. Vetrano, M. Rescigno, M.R. Cera, C. Correale, C. Rumio, A. Doni, et al., Unique role of junctional adhesion molecule-A in maintaining mucosal homeostasis in inflammatory bowel disease, Gastroenterology 135 (2008) 173–184.
[42] K.R. Groschwitz, R. Ahrens, H. Osterfeld, M.F. Gurish, X.N. Han, M. Abrink, et al., Mast cells regulate homeostatic intestinal epithelial migration and barrier function by a chymase/Mcpt4-dependent mechanism, Proc. Natl. Acad. Sci. U. S. A. 106 (2009) 22381–22386.
[43] H. Laroui, D. Geem, B. Xiao, E. Viennois, P. Rakhya, T. Denning, et al., Targeting intestinal inflammation with CD98 siRNA/PEI-loaded nanoparticles, Mol. Ther. 22 (2014) 69–80.
[44] T.T.N. Hang, G. Dalmasso, L. Torkvist, J. Halfvarson, Y.T. Yan, H. Laroui, et al., CD98 expression modulates intestinal homeostasis, inflammation, and colitis-associated cancer in mice, J. Clin. Invest. 121 (2011) 1733–1747.
[45] R. Francescone, V. Hou, S.I. Grivennikov, Cytokines, IBD, and colitis-associated cancer, Inflamm. Bowel Dis. 21 (2015) 409–418.
[46] L.W. Peterson, D. Artis, Intestinal epithelial cells: regulators of barrier function and immune homeostasis, Nat. Rev. Immunol. 14 (2014) 141–153.
[47] F. Yan, H.W. Cao, T.L. Cover, R. Whitehead, M.K. Washington, D.B. Polk, Soluble proteins produced by probiotic bacteria regulate intestinal epithelial cell survival and growth, Gastroenterology 132 (2007) 562–575.
[48] K.J. Maloy, F. Powrie, Intestinal homeostasis and its breakdown in inflammatory bowel disease, Nature 474 (2011) 298–306.
[49] R. Marouga, S. David, E. Hawkins, The development of the DIGE system: 2D fluorescence difference gel analysis technology, Anal. Bioanal. Chem. 382 (2005) 669–678.
[50] D.G. Kakhniashvili, N.B. Griko, L.A. Bulla, S.R. Goodman, The proteomics of sickle cell disease: profiling of erythrocyte membrane proteins by 2D-DIGE and tandem mass spectrometry, Exp. Biol. Med. 230 (2005) 787–792.
[51] G. Leoni, P.A. Neumann, N. Kamaly, M. Quiros, H. Nishio, H.R. Jones, et al.,

Annexin A1-containing extracellular vesicles and polymeric nanoparticles promote epithelial wound repair, J. Clin. Invest. 125 (2015) 1215–1227.
[52] S.E. Headland, H.R. Jones, L.V. Norling, A. Kim, P.R. Souza, E. Corsiero, et al., Neutrophil-derived microvesicles enter cartilage and protect the joint in inflammatory arthritis, Sci. Transl. Med. 7 (2015) 315ra190.
[53] N.K. Saxena, L. Taliaferro-Smith, B.B. Knight, D. Merlin, F.A. Anania, R.M. O'Regan, et al., Bidirectional crosstalk between leptin and insulin-like growth Factor-I signaling promotes invasion and migration of breast cancer cells via transactivation of epidermal growth factor receptor, Cancer Res. 68 (2008) 9712–9722.
[54] S.Y. Yang, J.Y. Chen, D. Zhao, D.E. Han, X.J. Chen, Comparative study on preparative methods of DC-Chol/DOPE liposomes and formulation optimization by determining encapsulation efficiency, Int. J. Pharm. 434 (2012) 155–160.
[55] B. Chassaing, G. Srinivasan, M.A. Delgado, A.N. Young, A.T. Gewirtz, M. Vijay-Kumar, Fecal lipocalin 2, a sensitive and broadly dynamic non-invasive biomarker for intestinal inflammation, PLoS One 7 (2012) e44328.
[56] N.J. Davidson, M.W. Leach, M.M. Fort, L. Thompson-Snipes, R. Kühn, W. Müller, et al., T helper cell 1-type CD4^{+} T cells, but not B cells, mediate colitis in interleukin 10-deficient mice, J. Exp. Med. 184 (1996) 241–251.
[57] R. Kuhn, J. Lohler, D. Rennick, K. Rajewsky, W. Muller, Interleukin-10-Deficient mice develop chronic enterocolitis, Cell 75 (1993) 263–274.
[58] E. Viennois, M.T. Baker, B. Xiao, L.X. Wang, H. Laroui, D. Merlin, Longitudinal study of circulating protein biomarkers in inflammatory bowel disease, J. Proteomics 112 (2015) 166–179.
[59] J. Dupaul-Chicoine, G. Yeretssian, K. Doiron, K.S.B. Bergstrom, C.R. McIntire, P.M. LeBlanc, et al., Control of intestinal homeostasis, colitis, and colitis-associated colorectal cancer by the inflammatory caspases, Immunity 32 (2010) 367–378.
[60] M. De Robertis, E. Massi, M.L. Poeta, S. Carotti, S. Morini, L. Cecchetelli, et al., The AOM/DSS murine model for the study of colon carcinogenesis: from pathways to diagnosis and therapy studies, J. Carcinog. 10 (2011) 9.
[61] H. Kawasaki, D.C. Altieri, C.D. Lu, M. Toyoda, T. Tenjo, N. Tanigawa, Inhibition of apoptosis by survivin predicts shorter survival rates in colorectal cancer, Cancer Res. 58 (1998) 5071–5074.
[62] B.M. Wiczer, G. Thomas, Phospholipase D and mTORC1: nutrients are what bring them together, Sci. Signal 5 (2012).
[63] M. Record, Exosome-like nanoparticles from food: protective nanoshuttles for bioactive cargo, Mol. Ther. 21 (2013) 1294–1296.
[64] P.K. Deol, I.P. Kaur, Improving the therapeutic efficiency of ginger extract for treatment of colon cancer using a suitably designed multiparticulate system, J. Drug Target 21 (2013) 855–865.
[65] C.Y. Hsiang, H.Y. Lo, H.C. Huang, C.C. Li, S.L. Wu, T.Y. Ho, Ginger extract and zingerone ameliorated trinitrobenzene sulphonic acid-induced colitis in mice via modulation of nuclear factor-kappa B activity and interleukin-1 beta signalling pathway, Food Chem. 136 (2013) 170–177.
[66] S. Prasad, A.K. Tyagi, Ginger and its constituents: role in prevention and treatment of gastrointestinal cancer, Gastroenterol. Res. Pract. 2015 (2015) 142179.
[67] M.P. Utrilla, M.J. Peinado, R. Ruiz, A. Rodriguez-Nogales, F. Algieri, M.E. Rodriguez-Cabezas, et al., Pea (Pisum sativum L.) seed albumin extracts show anti-inflammatory effect in the DSS model of mouse colitis, Mol. Nutr. Food Res. 59 (2015) 807–819.
[68] I. Fasolino, A.A. Izzo, T. Clavel, B. Romano, D. Haller, F. Borrelli, Orally administered allyl sulfides from garlic ameliorate murine colitis, Mol. Nutr. Food Res. 59 (2015) 434–442.
[69] R. Noubade, K. Wong, N. Ota, S. Rutz, C. Eidenschenk, P.A. Valdez, et al., NRROS negatively regulates reactive oxygen species during host defence and autoimmunity, Nature 509 (2014) 235–239.
[70] E. Rath, D. Haller, Mitochondria at the interface between danger signaling and metabolism: role of unfolded protein responses in chronic inflammation, Inflamm. Bowel Dis. 18 (2012) 1364–1377.
[71] M. Khounlotham, W. Kim, E. Peatman, P. Nava, O. Medina-Contreras, C. Addis, et al., Compromised intestinal epithelial barrier induces adaptive immune compensation that protects from colitis, Immunity 37 (2012) 563–573.
[72] S. Barrientos, O. Stojadinovic, M.S. Golinko, H. Brem, M. Tomic-Canic, Growth factors and cytokines in wound healing, Wound Repair Regen. 16 (2008) 585–601.
[73] R. Kamekura, P. Nava, M.L. Feng, M. Quiros, H. Nishio, D.A. Weber, et al., Inflammation-induced desmoglein-2 ectodomain shedding compromises the mucosal barrier, Mol. Biol. Cell 26 (2015) 3165–3177.
[74] S. Parkkila, A.K. Parkkila, T. Juvonen, H. Rajaniemi, Distribution of the carbonic-anhydrase Isoenzyme-I, isoenzyme-II, and isoenzyme-Vi in the human alimentary-tract, Gut 35 (1994) 646–650.
[75] J.L. Coombes, K.R.R. Siddiqui, C.V. Arancibia-Carcamo, J. Hall, C.M. Sun, Y. Belkaid, et al., A functionally specialized population of mucosal CD103(+) DCs induces Foxp3(+) regulatory T cells via a TGF-beta- and retinoic acid-dependent mechanism, J. Exp. Med. 204 (2007) 1757–1764.
[76] H. Yamanishi, H. Murakami, Y. Ikeda, M. Abe, T. Kumagi, Y. Hiasa, et al., Regulatory dendritic cells pulsed with carbonic anhydrase I protect mice from colitis induced by CD4(+)CD25(-) T cells, J. Immunol. 188 (2012) 2164–2172.
[77] K. Mori, H. Yamanishi, Y. Ikeda, T. Kumagi, Y. Hiasa, B. Matsuura, et al., Oral administration of carbonic anhydrase I ameliorates murine experimental colitis induced by Foxp3(-)CD4(+)CD25(-) T cells, J. Leukoc. Biol. 93 (2013) 963–972.
[78] M. Kitano, M. Kudo, K. Yamao, T. Takagi, H. Sakamoto, T. Komaki, et al., Characterization of small solid tumors in the pancreas: the value of contrast-enhanced harmonic endoscopic ultrasonography, Am. J. Gastroenterol. 107 (2012) 303–310.
[79] J. Terzic, S. Grivennikov, E. Karin, M. Karin, Inflammation and colon cancer, Gastroenterology 138 (2010) 2101–2114.
[80] D.C. Rubin, A. Shaker, M.S. Levin, Chronic intestinal inflammation: inflammatory bowel disease and colitis-associated colon cancer, Front. Immunol. 3 (2012) 107.
[81] J.C. Arthur, E. Perez-Chanona, M. Muhlbauer, S. Tomkovich, J.M. Uronis, T.J. Fan, et al., Intestinal inflammation targets cancer-inducing activity of the microbiota, Science 338 (2012) 120–123.
[82] J. Liang, M. Nagahashi, E.Y. Kim, K.B. Harikumar, A. Yamada, W.C. Huang, et al., Sphingosine-1-Phosphate links persistent STAT3 activation, chronic intestinal inflammation, and development of colitis-associated cancer, Cancer Cell 23 (2013) 107–120.
[83] G. Rogler, Chronic ulcerative colitis and colorectal cancer, Cancer Lett. 345 (2014) 235–241.
[84] I.K. Kwon, R. Wang, M. Thangaraju, H. Shuang, K. Liu, R. Dashwood, et al., PKG inhibits TCF signaling in colon cancer cells by blocking beta-catenin expression and activating FOXO4, Oncogene 29 (2010) 3423–3434.
[85] D.D. Browning, I.K. Kwon, R. Wang, cGMP-dependent protein kinases as potential targets for colon cancer prevention and treatment, Future Med. Chem. 2 (2010) 65–80.
[86] S.R. Li, V.G. Gyselman, S. Dorudi, S.A. Bustin, Elevated levels of RanBP7 mRNA in colorectal carcinoma are associated with increased proliferation and are similar to the transcription pattern of the proto-oncogene c-myc, Biochem. Biophys. Res. Commun. 271 (2000) 537–543.
[87] R. Hrabakova, M. Kollareddy, J. Tyleckova, P. Halada, M. Hajduch, S.J. Gadher, et al., Cancer cell resistance to aurora kinase inhibitors: identification of novel targets for cancer therapy, J. Proteome Res. 12 (2013) 455–469.
[88] Y. Lin, P.J. Buckhaults, J.R. Lee, H.R. Xiong, C. Farrell, R.H. Podolsky, et al., Association of the actin-binding protein transgelin with lymph node metastasis in human colorectal cancer, Neoplasia 11 (2009), 864–U209.
[89] M. Yeo, D.K. Kim, H.J. Park, T.Y. Oh, J.H. Kim, S.W. Cho, et al., Loss of transgelin in repeated bouts of ulcerative colitis-induced colon carcinogenesis, Proteomics 6 (2006) 1158–1165.